HydroNumerics

HydroNumerics

Crib Point LNG Facility

Hydrodynamic Modelling Report

Appendix A
Hydrodynamic Model

June 2020

Prepared for CEE Pty Ltd

HydroNumerics Pty Ltd
ABN 87 142 999 246
www.hydronumerics.com.au

NOTICE

DISCLAIMER

The accuracy of information presented in this document is entirely dependent on the accuracy and completeness of supplied information. Hydronumerics Pty Ltd makes no warranty, representation or guarantee with respect to the accuracy and completeness of supplied information, shall have no liability to any person for any errors or omissions in the supplied information, and shall have no liability for loss or damage of any kind suffered or incurred by any person acting in reliance on the information in this document where the loss or damage arises from errors or omissions in the supplied information.

HydroNumerics

CONTENTS

1 AEM3D Technical Specifications 1

1.1 Code Overview 1
1.2 Hydrodynamic Processes 1
1.3 Mixing Model 2
1.3.1 Introduction 2
1.3.2 Energy terms in the mixed layer model 2
1.3.3 Mixing Timestep 2
1.3.4 Parameterisations 3

2 Model Bathymetry 7

2.1 Comparison Between Data Sets 7
2.2 Cross-sections of model grid at Crib Point Jetty. 10

3 Model Performance 14

3.1 Calibration Results 14
3.1.1 Overview 14
3.1.2 Simulation A, 50 x 50 m grid 15
3.1.3 Simulation P, 20 x 20 m grid 22
3.1.4 Simulation X, 50 x 50 m grid 29

1 AEM3D Technical Specifications

1.1 Code Overview

Source Code	Fortran 2008
Operating Systems	Windows XP above (32 or 64bit) Mac OSX 10.7+ Linux (32 or 64bit)
Output Format	NetCDF

1.2 Hydrodynamic Processes

Horizontal Grid	Varying width orthogonal
Vertical coordinate	z
Grid stencil	Arakawa C-grid
Equation of state	UNESCO
Free surface solution	Mode-split conjugate gradient method (Casulli and Cheng, 1992)
Momentum solution	Semi implicit Euler Lagrange Method (Casulli and Cheng, 1992)
Scalar Transport	ULTIMATE-QUICKEST (Leonard, 1991)
Turbulence closure	TKE base vertical mixing model (Hodges et al, 2000)
Wind momentum	Stress boundary condition at the free surface
Bottom and sidewall boundary conditions	Options for no-slip, slip, drag and heterogenous maps for drag coeffcient
Surface thermodynamics	Sensible and latent heat fluxed with atmospheric stability correction.
Artificial mixers	Bubble plumes Jets/impellors Draft tubes

1.3 Mixing Model

1.3.1 Introduction

AEM3D models the vertical Reynolds stress terms (and thus the turbulent fluxes) in momentum and transport equations with a 3D mixed-layer approach derived from the mixing energy budgets developed for 1D lake modelling (Imberger and Patterson (1981), Spigel et al. (1986) , Imberger and Patterson (1990)). Whereas 1D mixed-layer models are typically Lagrangian, regridding the vertical domain to match the number of mixed regions in the water column, the present 3D method uses an Eulerian fixed-grid framework as Lagrangian 3D methods typically obtain highly skewed grid cells when horizontal gradients in mixing occur. The present model applies a separate 1D mixed-layer model to each water column to provide vertical turbulent transport, whereas 3D transport of TKE is used to provide the dynamic effect of 3D motions on the TKE available for vertical mixing.

1.3.2 Energy terms in the mixed layer model

To understand the present mixed-layer approach, it is useful to qualitatively define some of the energy fluxes. First, we can characterize four energy terms:

- The TKE available for mixing, TKE_A
- The TKE required for mixing, E_{req}
- The TKE dissipated, E_ε and
- The residual mixing energy, E_M.

Of these, only the last, which is effectively the sum of the others at the end of the mixing algorithm, is considered a transported variable. Second, it is useful to characterize two types of mixing events in a stratified fluid:

- convective mixing of unstable density gradients that decreases the potential energy of the fluid and releases TKE
- mixing of stable density gradients that dissipates TKE and increases potential energy.

The former is one of the TKE sources for mixing (TKE_A), whereas the latter is exactly the local energy required to mix (E_{req}). These two density gradient terms are computed from the vertical buoyancy scale, with the magnitude of a negative value providing the convective contribution to TKE_A and a positive value providing E_{req}. The distinction between the positive and negative forms of the buoyancy scale is critical to the model, as an unstable density gradient will always create TKE_A, whereas a stable gradient ($E_{req} > 0$) will consume TKE_A only when $TKE_A >= E_{req}$. Finally, we need a definition for a 'mixed layer'; this is taken to be a set of vertically contiguous grid cells that share the same density, scalar concentrations, and grid-scale velocity.

1.3.3 Mixing Timestep

A mixing model timestep for each column of water can be broken down in to the following steps

1. Calculate wind energy input, E_{wind}
2. Calculate bottom energy input, E_{drag}
3. For each column cycle from surface cell to bottom cell
4. Calculate generation of TKE by shear, E_{shear}

5. Calculate energy required for mixing, E_{req}
6. Calculate total energy available if two cells were totally mixed, TKE_{mixed}
7. Calculate time estimate for total mixing T_{TKE}
8. If unstable calculate time estimate based on convective overturn T_{conv}
9. Calculate mixing fraction η_f
10. If there is enough energy then mix cells
11. End of cycle from surface cell to bottom cell
12. Dissipate excess mixing energy

Details for each step are as follows:

1.3.4 Parameterisations

1. Wind Energy

Wind generation of TKE is parametrised as

$$E_{wind} = \frac{1}{2} C_n^3 dt u_*^3$$

Where u_* is the wind shear velocity given by

$$u_* = \sqrt{\frac{C_D^{wind} \rho_{air}}{\rho_0}} U_{wind}$$

and the mixing coefficient C_n is set to 1.33. The wind energy for each column is added to the available TKE of the surface cell.

2. Bottom Energy

TKE is also generated due to drag on the bottom. This energy is parametrised as

$$E_{drag} = C_b (|u_{bot}| + |v_{bot}|)^{3/2} dt$$

The bottom energy for each column is added to the available TKE of the bottom cell.

3. Cycle from surface to bottom

Once the external energy sources have been added to the surface and bottom cells the main mixing routine is called. This routine loops from the surface cell to the bottom cell and generates the mixing layers for the column.

The loop first sets the surface cell (k_{surf}) to a mixed layer and attempts to mix the cell k_{surf} -1 into this mixed layer. If there is enough energy to mix the cells and t is large enough for the cell to be fully mixed (ηf = 1) then the cells are mixed k_{surf}-1 is added to the mixed layer and then we attempt to mix k_{surf}-2 with the mixed layer. If there is not enough energy for mixing to occur or η_f < 1 then the mixed layer is closed, (k_{surf}-1) is set to a mixed layer and energy budgets are computed for k_{surf}-2. If there is enough energy for mixing to occur but the mixing fraction is < 1 then partial mixing occurs.

4. Shear Energy

Shear generation of TKE is parametrised as

$$E_{shear} = \frac{1}{2} C_s S^2 dz_l$$

the mixing coefficient C_s is set to 0.15 and S is the shear defined as

$$S^2 = (U_{ml} - U_l)^2 + (V_{ml} - V_l)^2$$

subscripts *ml* refer to values in the mixed layer and subscripts *l* refer to the cell directly below the mixed layer ie. the cell that we are checking to see if it will become part of the mixed layer. Shear energy is stored in the cell that is being mixed into the mixed layer.

5. Potential Energy

The energy required to mix the current cell into the mixed layer is given by

$$E_{req} = -g' dz_l dz_{ml}$$

where the reduced gravity term is given by

$$g' = \frac{1}{2} g(\rho_{ml} - \rho_l) \frac{dz_l dz_{ml}}{\rho_{ml}(dz_{ml} - dz_l)\rho_l}$$

dz_{ml} is the mixed layer depth given by the sum of all the dz of cells in the mixed layer.

6. Total Available TKE Energy

To determine a timescale for the mixing we first determine the total amount of energy if the cell of interest is completely mixed into the mixing layer. If the density profile is unstable then energy generated from convective overturns is added. The total TKE is then

$$TKE_{\text{mixed}} = \begin{cases} TKE_{ml} + TKE_l + E_{shear} : E_{req} \geq 0 \\ TKE_{ml} + TKE_l + E_{shear} - C_c E_{req} : E_{req} < 0 \end{cases}$$

the mixing coefficient C_C is set to 0.2. The TKE of the mixed layer (TKE_{ml}) and the cell (TKE_l) include energy from wind stirring and bottom drag as detailed above.

7. Timescale for mixing due to turbulence

To try and limit the time step dependence on mixing we introduce a timescale for the mixing to occur. If this timescale is larger than the timestep used then partial mixing occurs. The time scale due to turbulent mixing is given by

$$T_{turb} = C_{TT} dz_l \sqrt{\frac{C_s dz_{ml} + dz_l}{2TKE_{mixed}}}$$

the coefficient C_{TT} is set to 50.0.

8. Timescale for mixing due to convective overturn

If the density profile is unstable then we introduce a timescale for overturning.

$$T_{conv} = C_{TC} dz_l \sqrt{\frac{C_s dz_{ml} + dz_l}{g'}}$$

If the time scale for overturning is shorter than the timescale for mixing due to turbulence then we use this timescale to calculate our mixing fraction.

9. Calculate mixing fraction

The mixing fraction is simply the timestep t divided by the shorter of the two timescales. The mixing fraction is limited to 1.0.

$$n_f = \min\left(\frac{\Delta t}{\min\left(T_{turb}, T_{conv}\right)}, 1\right)$$

10. Energy Budget

Before any mixing takes place the mixing routine checks to see if there is sufficient TKE available to overcome the potential energy. If $TKE_{mixed} > \eta_f E_{req}$ the mixing takes place using the calculated mixing fraction. If $TKE_{mixed} < \eta_f E_{req}$ no mixing occurs, the available TKE is dissipated completely and the mixed layer is closed. For complete mixing any excess TKE (ie. TKE_{mixed} - E_{req}) is stored in the mixed layer and is included in the energy budget for the next layer. For partial mixing excess TKE is stored proportionally by volume in the mixed layer and the cell being mixed.

11. Mixing of cell into mixed layer

The mixing of cells depends on whether the cells are fully or partially mixed. If $n_f = 1$ all scalar and velocity values within the mixed layer are equal. Scalar concentrations are mixed by volume such that

$$C'_{ml} = \frac{C_{ml} dz_{ml} + C_l dz_l}{dz_{ml} + dz_l}$$

Where the C_{ml} is the scalar concentration of the mixed layer and C_l is the scalar concentration of the cell being mixed. The ‘ indicates the value after mixing.

Velocities are mixed my mass

$$U'_{ml} = \frac{\rho_{ml} U_{ml} dz_{ml} + \rho_l U_l dz_l}{\rho_{ml} dz_{ml} + \rho_l dz_l}$$

For partial mixing only the cell being mixed and the cell at the bottom of the mixed layer are modified.

$$C_k = \begin{cases} C_{ml} : \ k = k_l + 2 : k_{ml-top} \\ \left(1 - n_f\right) C_{ml} + n_f \dfrac{C_{ml} dz_{ml} + C_l dz_l}{dz_{ml} + dz_l} : k = k_l + 1 \\ \left(1 - n_f\right) C_l + n_f \dfrac{C_{ml} dz_{ml} + C_l dz_l}{dz_{ml} + dz_l} : \ k = k_l \end{cases}$$

An analogous expression is used for partial mixing of velocity.

12. Dissipation of energy

After the mixing of cells has concluded excess energy is dissipated according to

$$TKE = TKE - \frac{1}{2} C_\epsilon \Delta t \left(\frac{TKE}{dz}\right)^{3/2}$$

where C_ϵ is the dissipation coefficient. Any TKE left after dissipation is then transported by the scalar transport routine before becoming available for mixing in the following timestep.

2 Model Bathymetry

2.1 Comparison Between Data Sets

Bathymetric datasets that used to develop the model grid were:

- Victorian Coastline DEM (VCDEM) raster data at 10 m resolution from Spatial Systems CRC – used for depths shallower than 30 mAHD;
- Bass Strait Depth Zone Contour Lines (BSDZCL) from the 1:250,000 National Bathymetric Map Series from DELWP – used for depths greater than and equal to 30 m AHD; and
- Western Port DEM (WPDEM) raster data at 2.5 m resolution from Frontier SI (formerly Spatial Systems CRC) – used for Crib Point region.

A 0.5 m resolution bathymetric dataset for the region around Berth 2 at Crib Point Jetty was provided by the VRCA. Figure 2.1 and Figure 2.2 show a comparison of WP-DEM and VRCA0044 bathymetric data. These data were interpolated onto a 2 m grid and the VRCA0044 interpolation subtracted from the WP-DEM to show differences in the datasets (Figure 2.3). Longitudinal bands of 10-30 cm deficit or surfeit are evident in the difference plot, perhaps due to regions where accretion or erosion has occurred between bathymetric surveys.

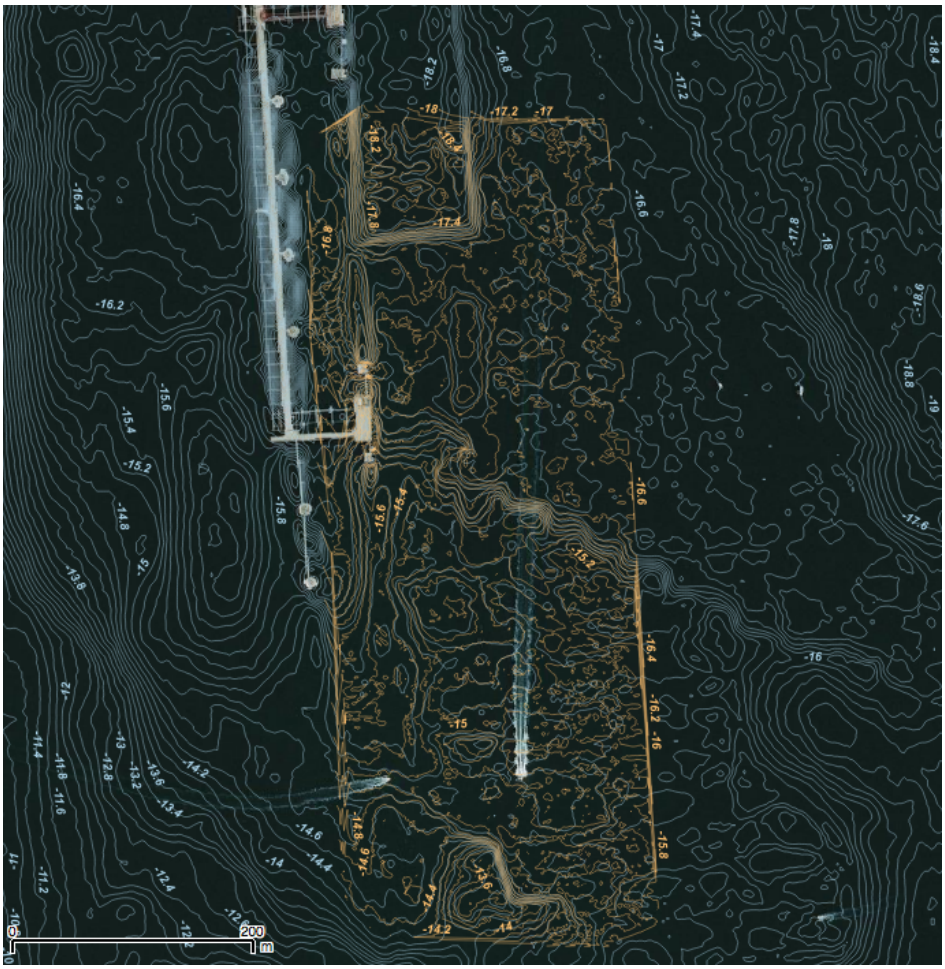

Figure 2.1 Bathymetric contours from Westernport 2.5 m DEM (blue) and VRCA0044 0.5 m (orange) data.

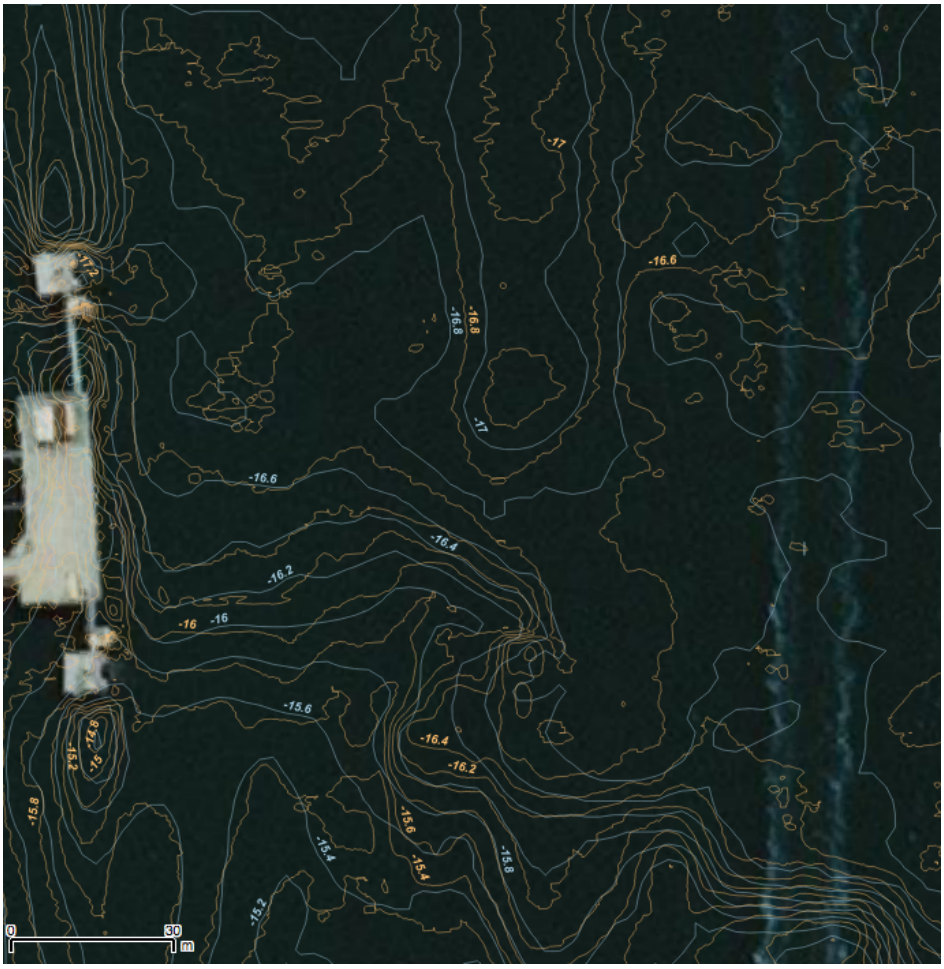

Figure 2.2 Bathymetric contours from Westernport 2.5 m DEM (blue) and VRCA0044 0.5 m (orange) data.

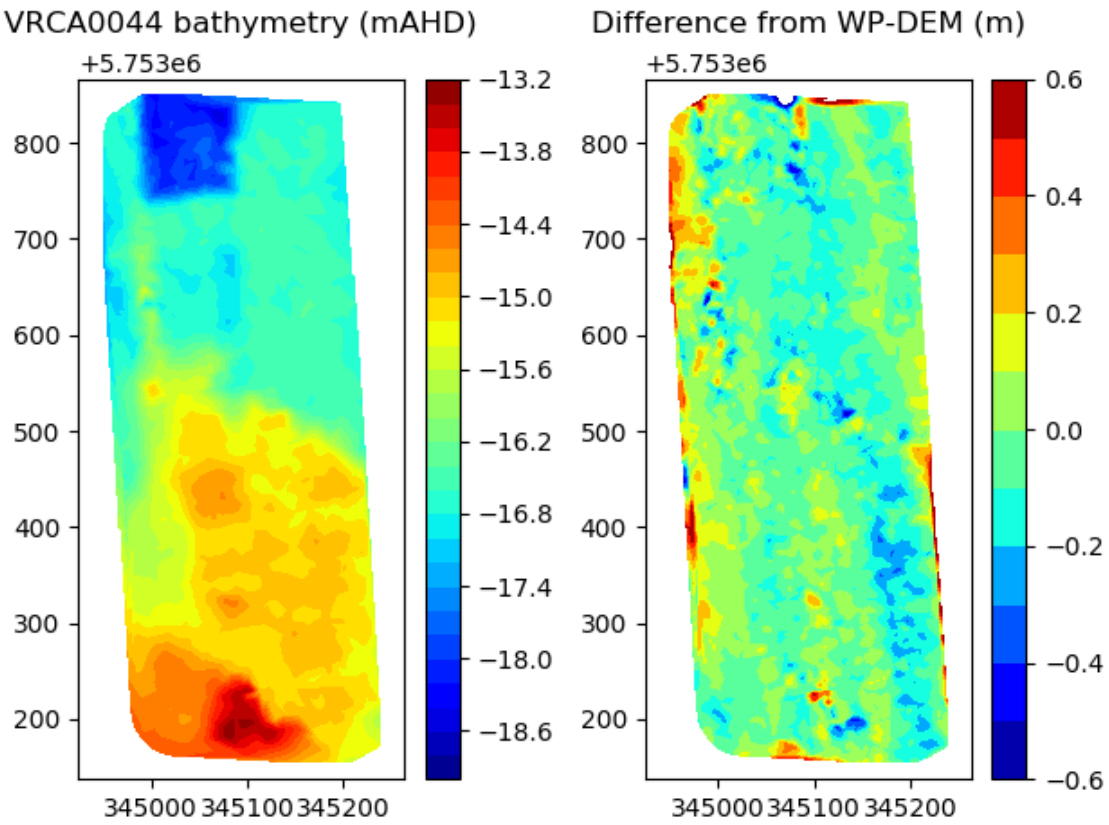

Figure 2.3 VRCA0044 0.5 m bathymetric data (left) and the difference between this data and the Westernport 2.5 m DEM bathymetric data (right) when interpolated on a 2 m grid.

2.2 Cross-sections of model grid at Crib Point Jetty.

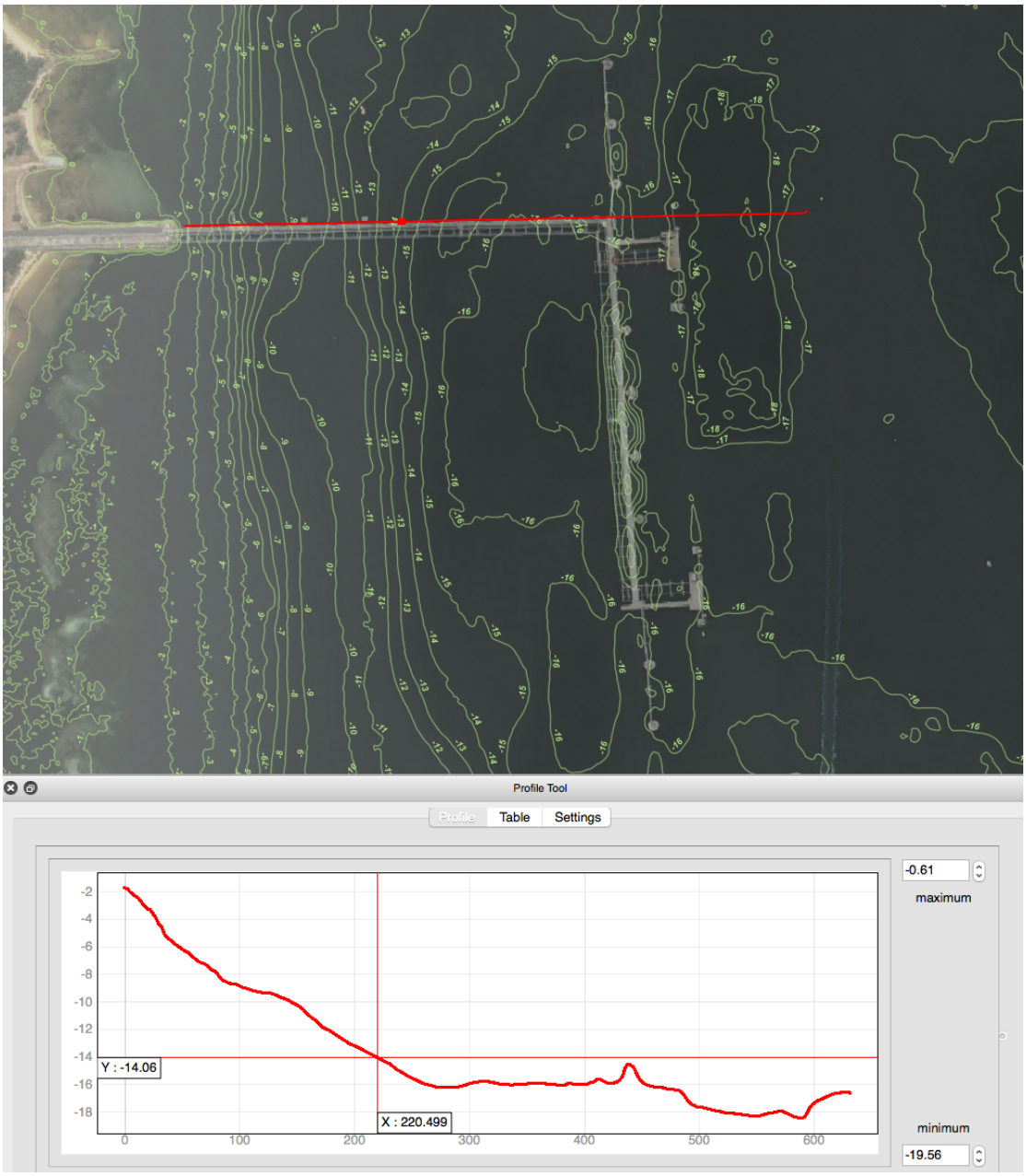

Figure 2.4 Cross-section along north side of E-W jetty arm.

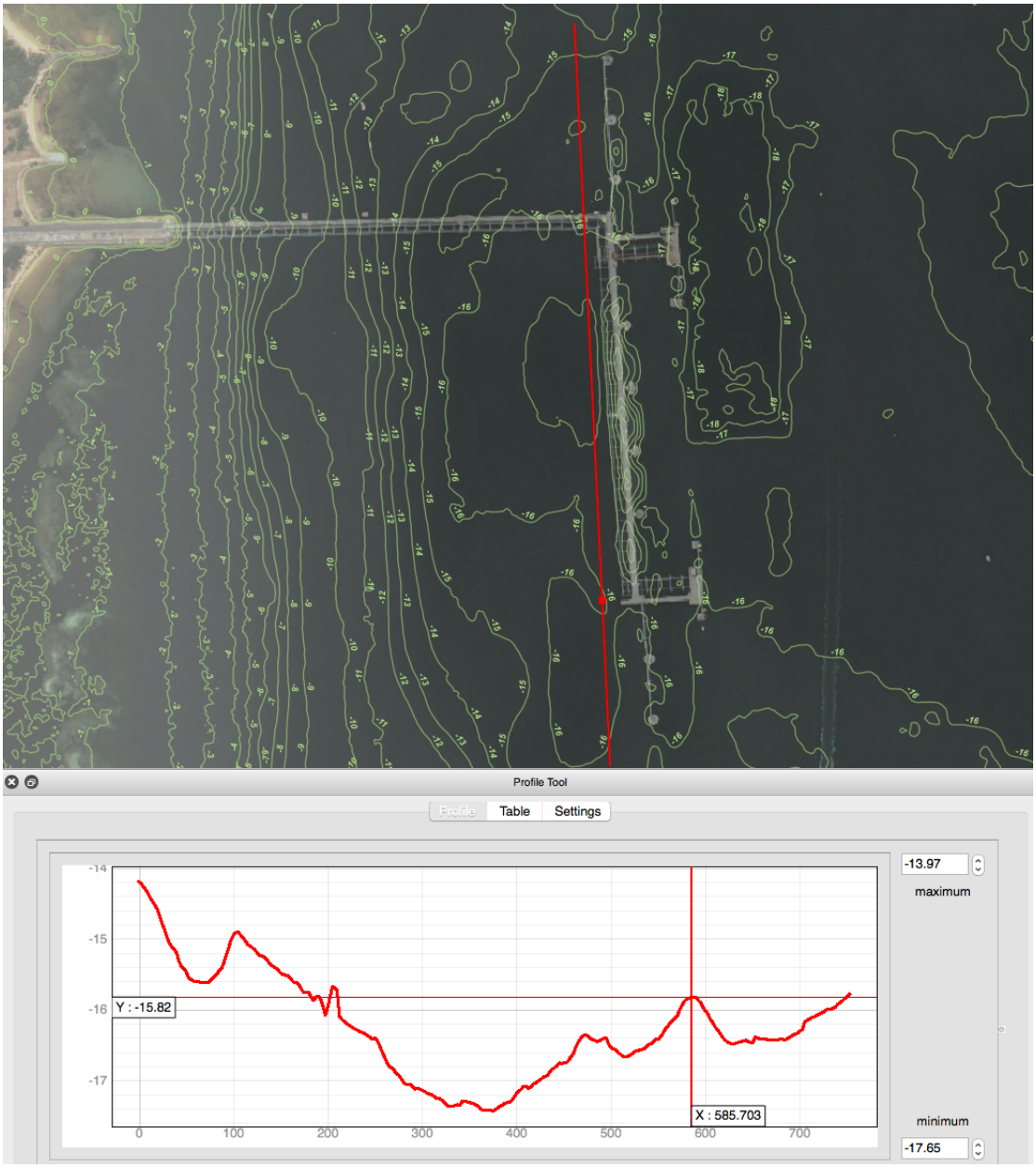

Figure 2.5 Cross-section along west side of N-S jetty arm.

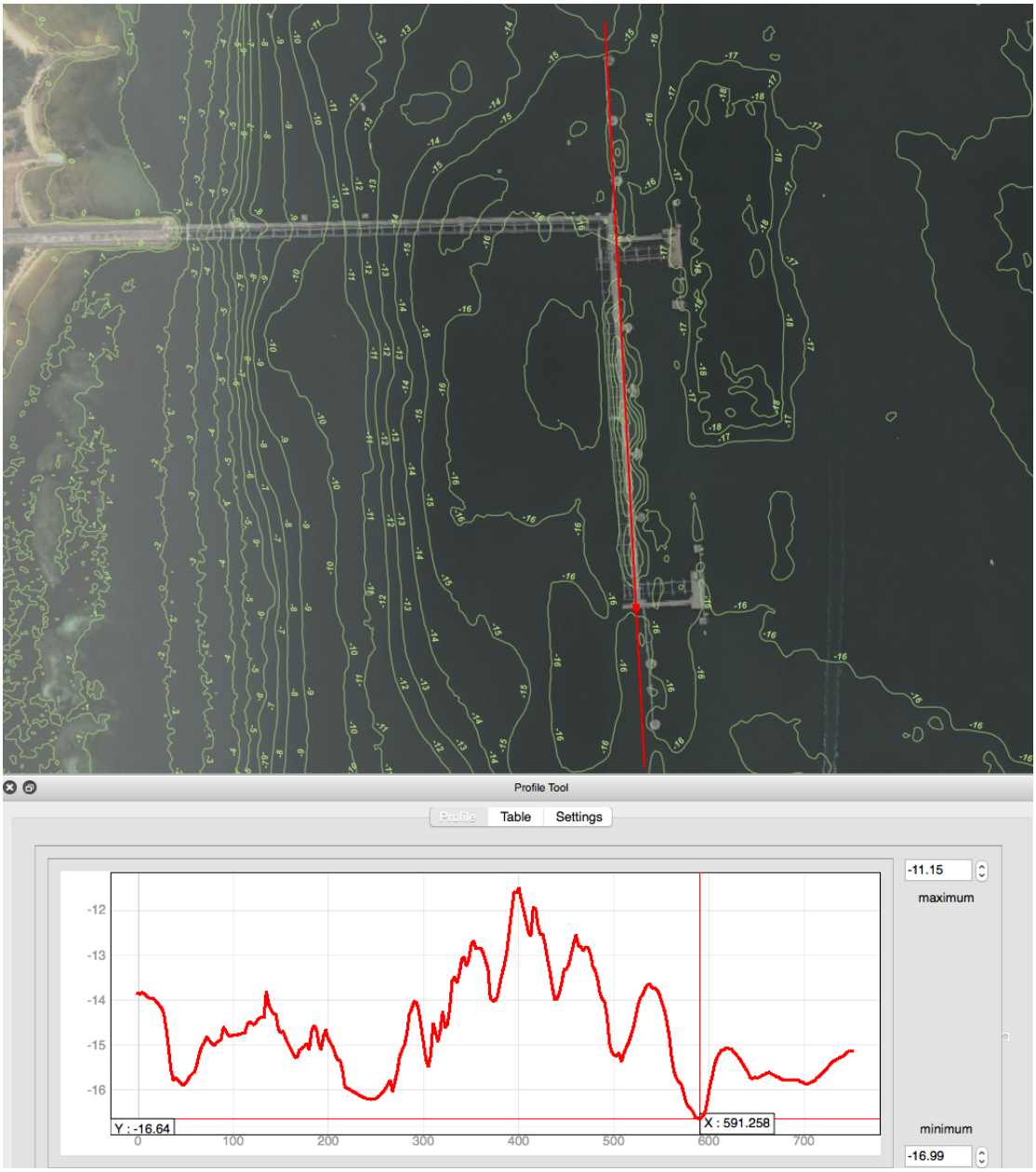

Figure 2.6 Cross-section along beneath N-S jetty arm.

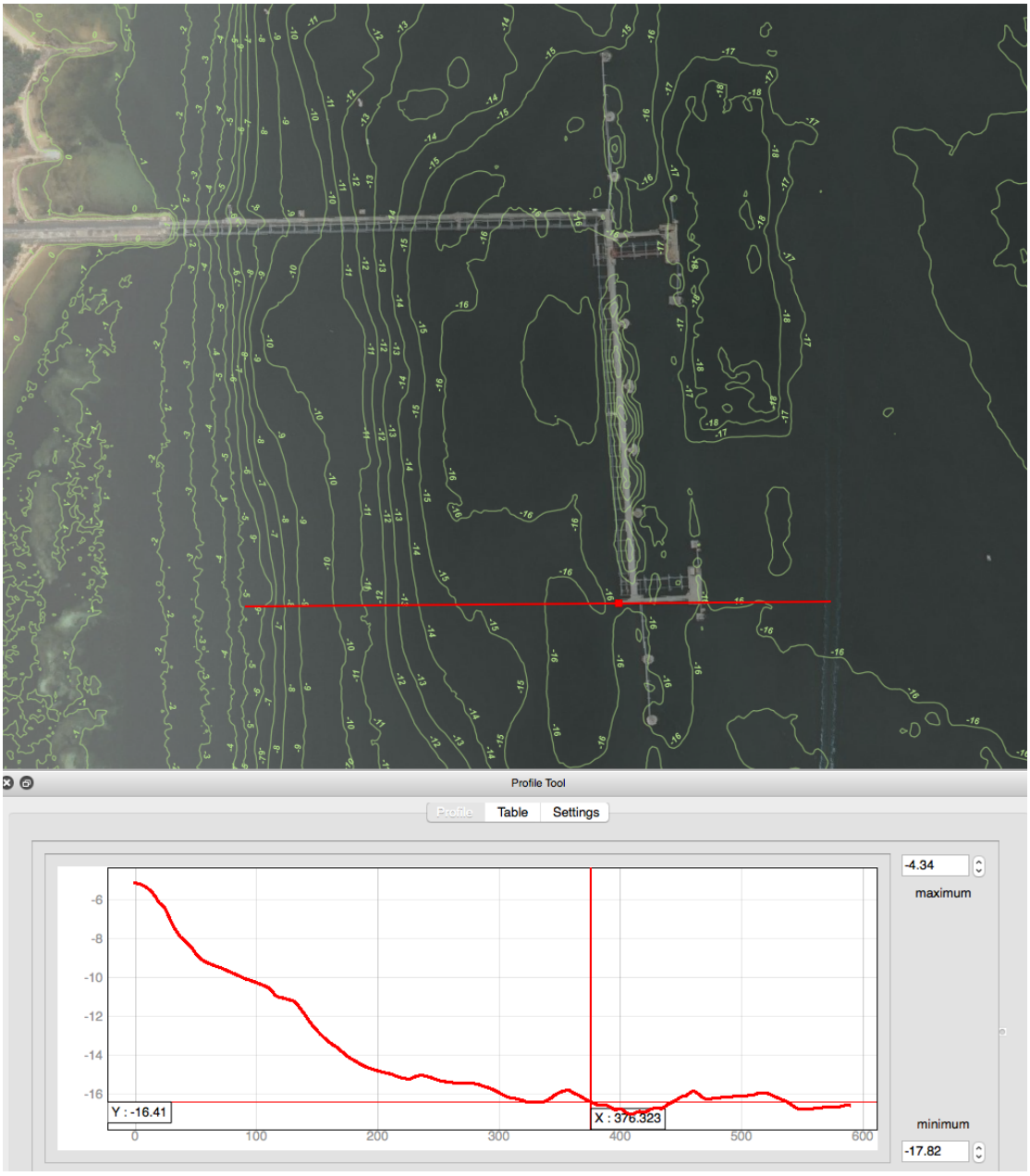

Figure 2.7 E-W cross-section along at southern end of N-S jetty arm.

3 Model Performance

3.1 Calibration Results

3.1.1 Overview

The sections below illustrate the model performance for a sub-set of model configurations that were used for the FSRU assessments. These are:

- Simulation A: Constant moderate drag (C_D = 5 x 10^{-3}), high dissipation (C_ϵ = 1.15), slow vertical mixing (C_{TT} = 50);
- Simulation P: Drag map (5 x 10^{-5} < C_D < 0.25), low dissipation (C_ϵ = 0.018), slow vertical mixing (C_{TT} = 50). The drag map applied is illustrated in Figure 3.1 below; and
- Simulation X: Constant low drag (C_D = 2 x 10^{-3}), high dissipation (C_ϵ = 1.15), rapid vertical mixing (C_{TT} = 8).

Results from simulation P with a 50 x 50m grid near Crib Point are illustrated in the main body of the report. Results from a 20 x 20 m grid simulation of the same are shown in Section 3.1.3 below.

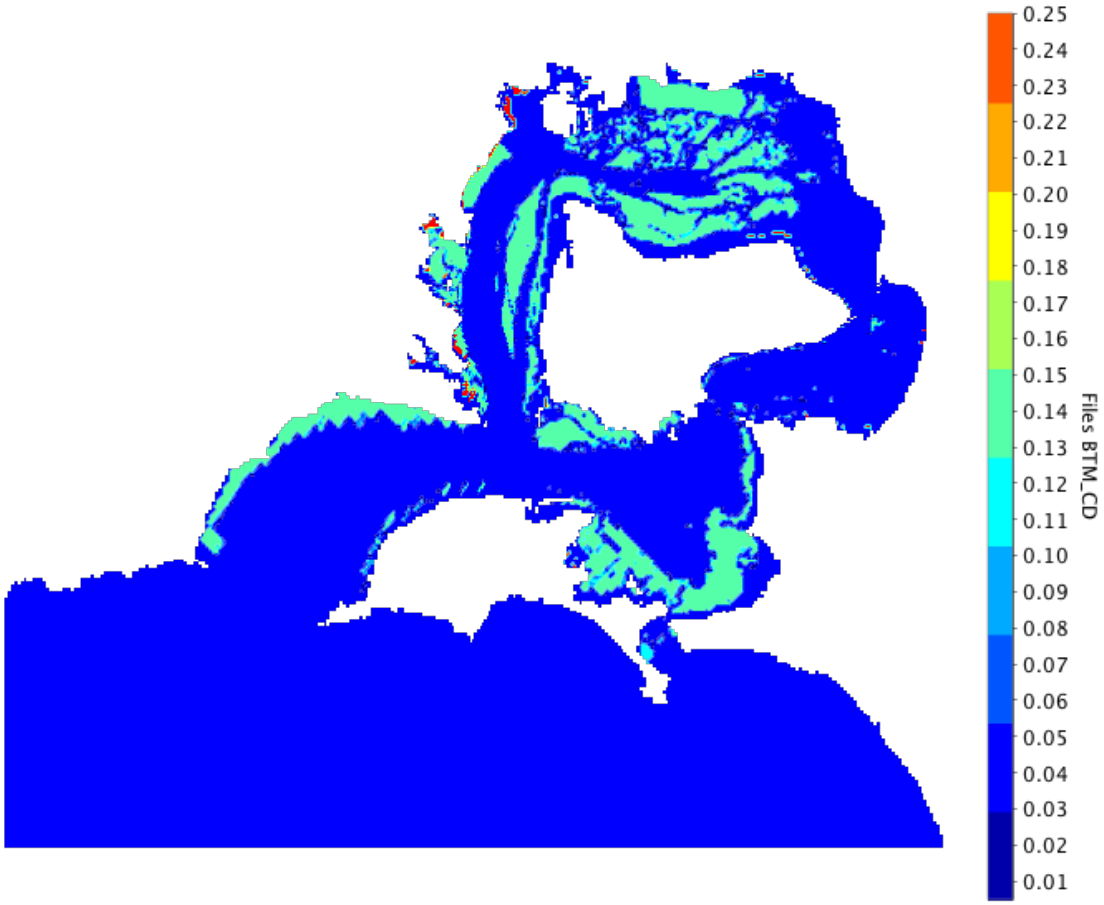

Figure 3.1 Map of bottom drag coefficient. Blue indicated low drag bare bed, green indicated seagrass meadows and red indicates mangrove stands.

3.1.2 Simulation A, 50 x 50 m grid

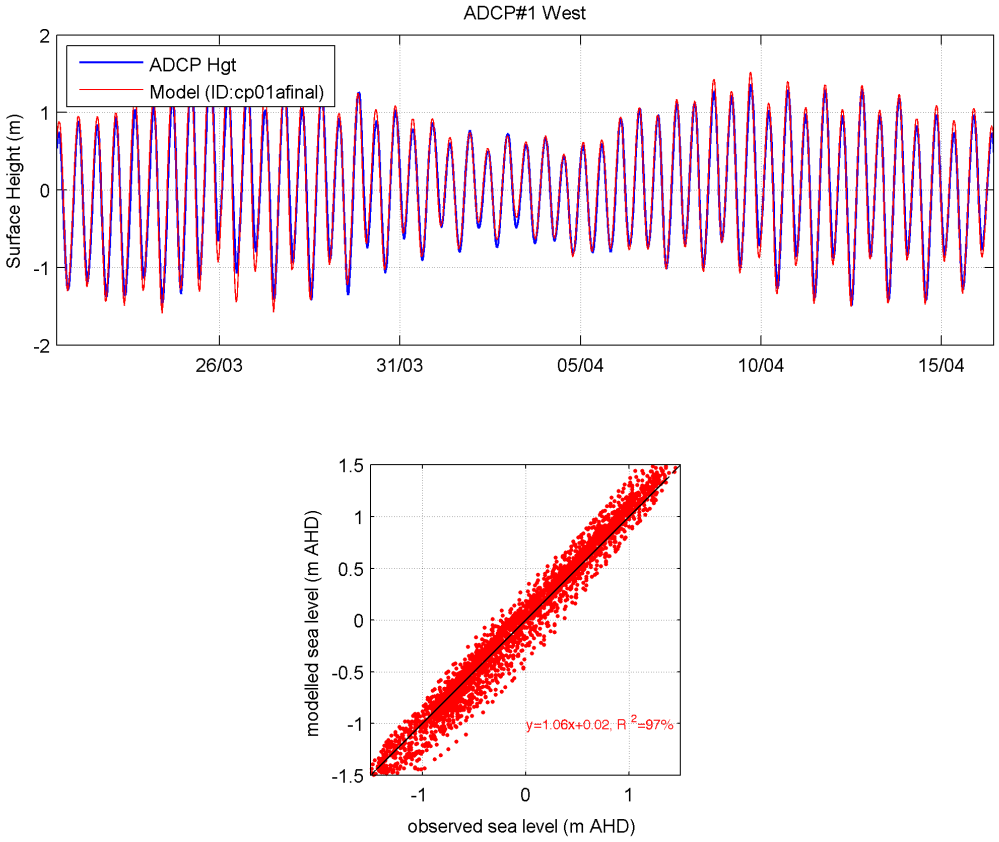

Figure 3.2 Comparison between observed (blue) and modelled (red) surface heights at West ADCP 1 (West).

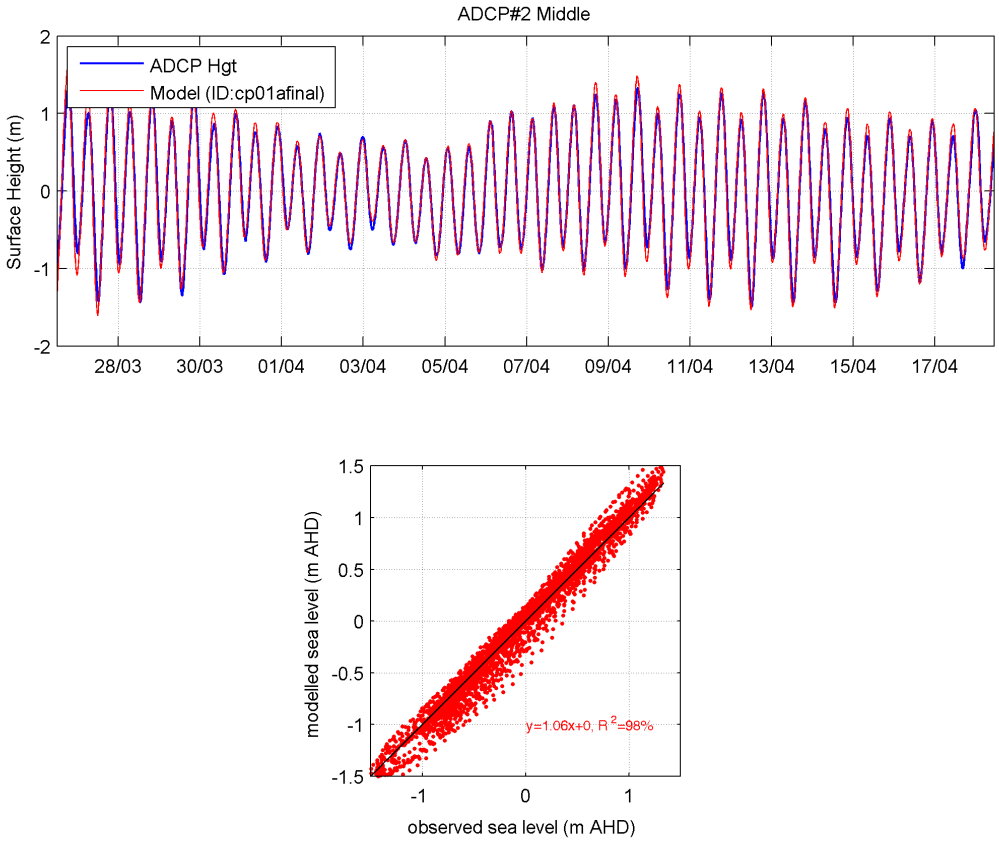

Figure 3.3 Comparison between observed (blue) and modelled (red) surface heights at middle ADCP 2 (Middle).

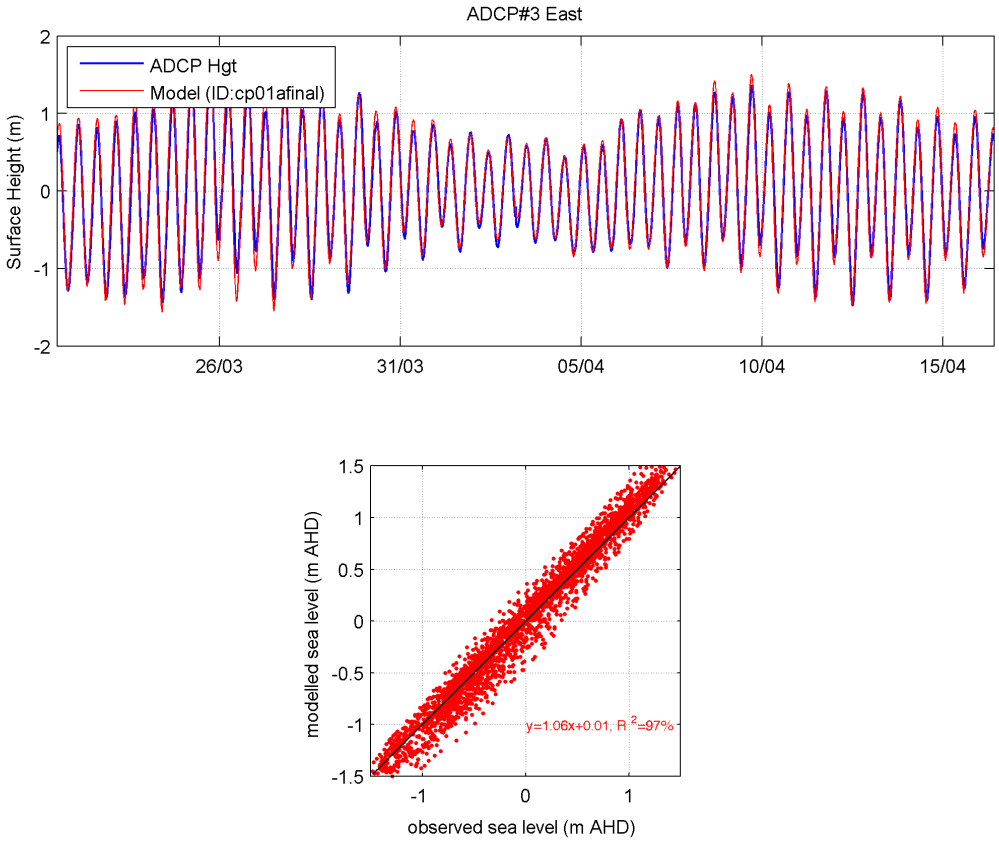

Figure 3.4 Comparison between observed (blue) and modelled (red) surface heights at East ADCP 3 (East).

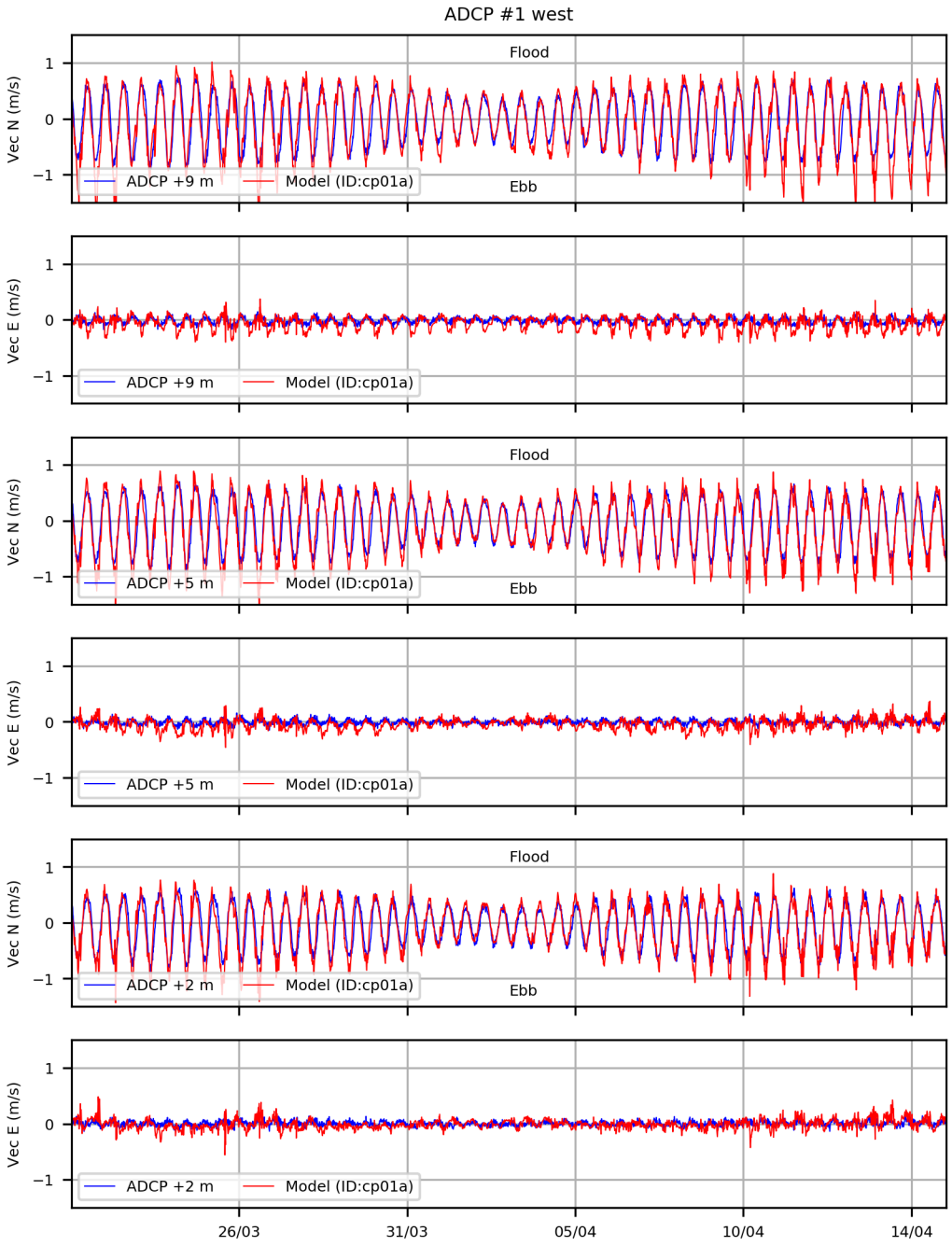

Figure 3.5 Comparison between observed (blue) and modelled (red) north and east current vectors at ADCP 1 (West).

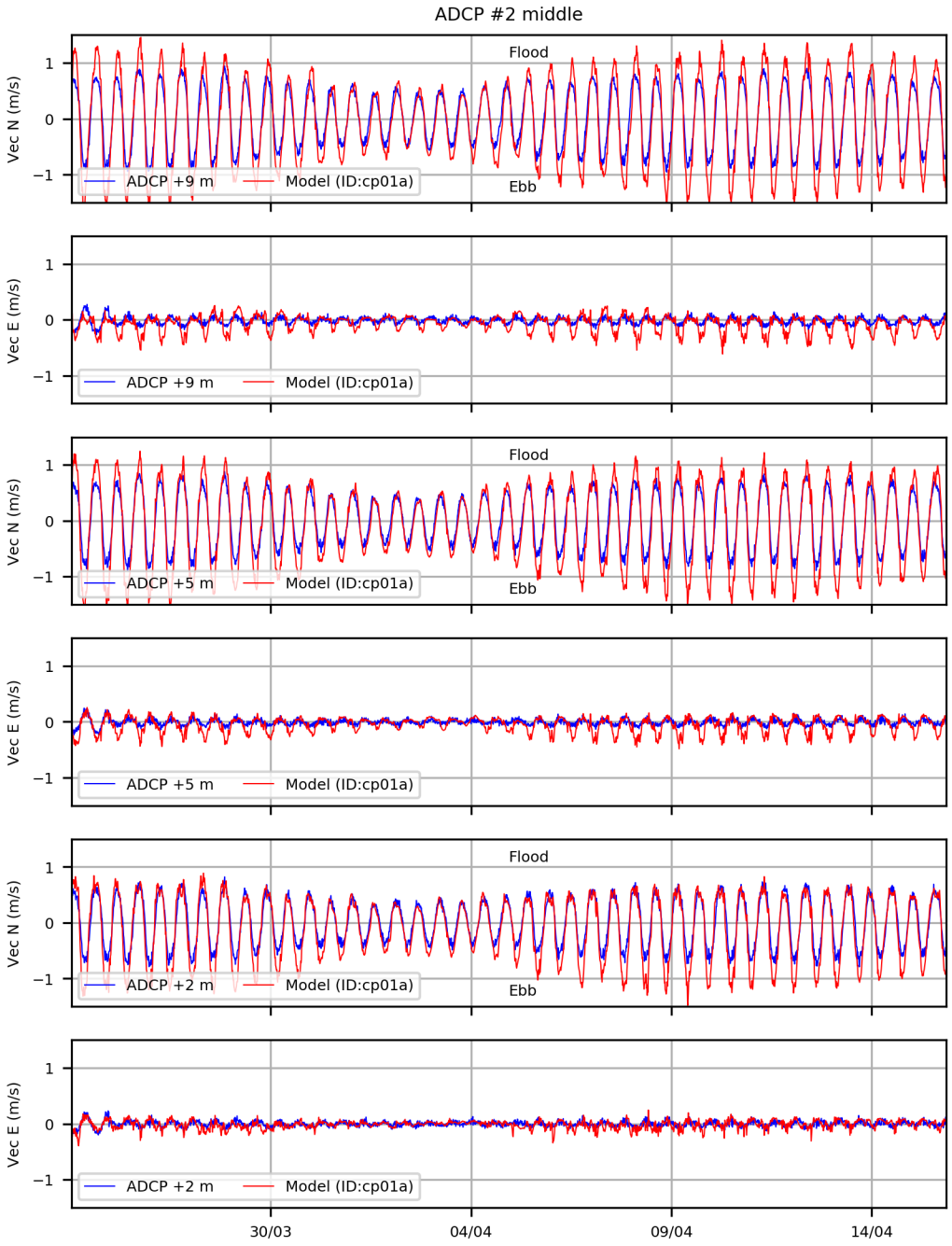

Figure 3.6 Comparison between observed (blue) and modelled (red) north and east current vectors at ADCP 2 (Middle).

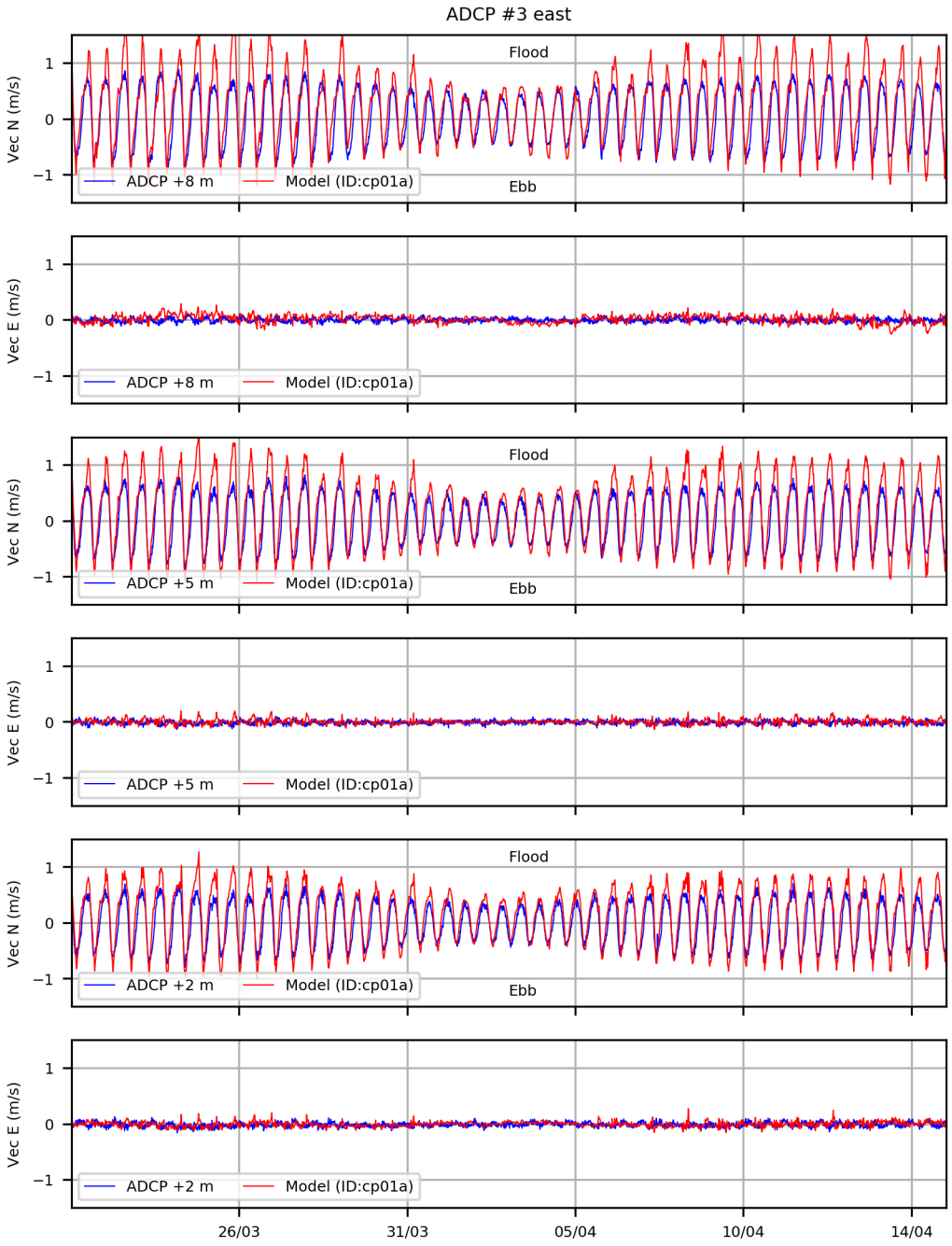

Figure 3.7 Comparison between observed (blue) and modelled (red) north and east current vectors at ADCP 3 (East).

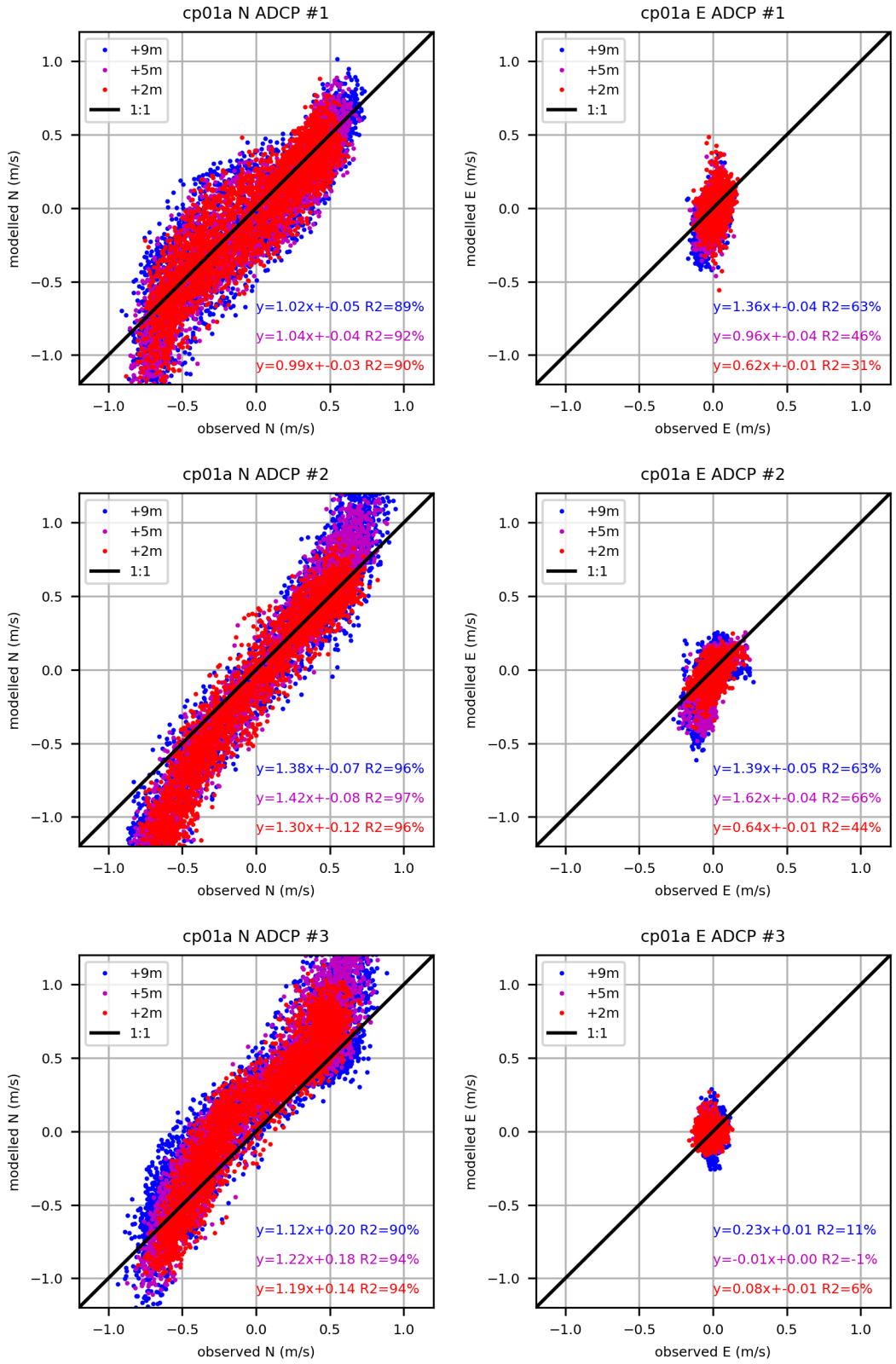

Figure 3.8 Least squares linear fits observed and modelled north and east current vectors at all three ADCP locations.

3.1.3 Simulation P, 20 x 20 m grid

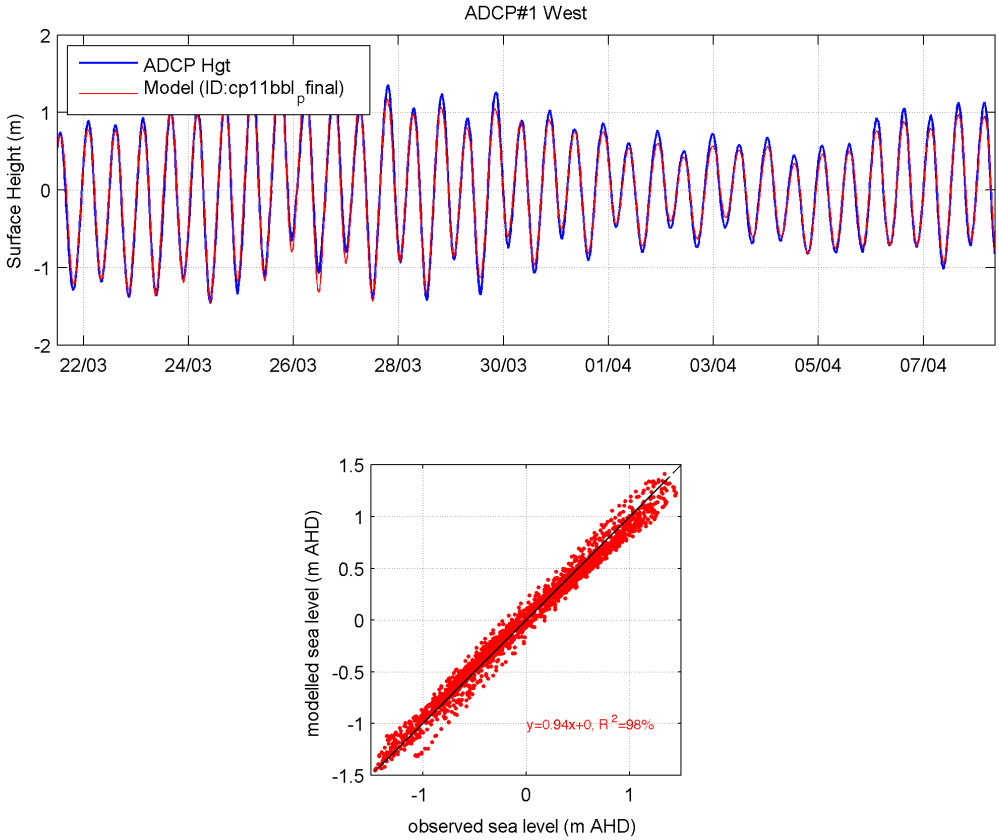

Figure 3.9 Comparison between observed (blue) and modelled (red) surface heights at West ADCP 1 (West).

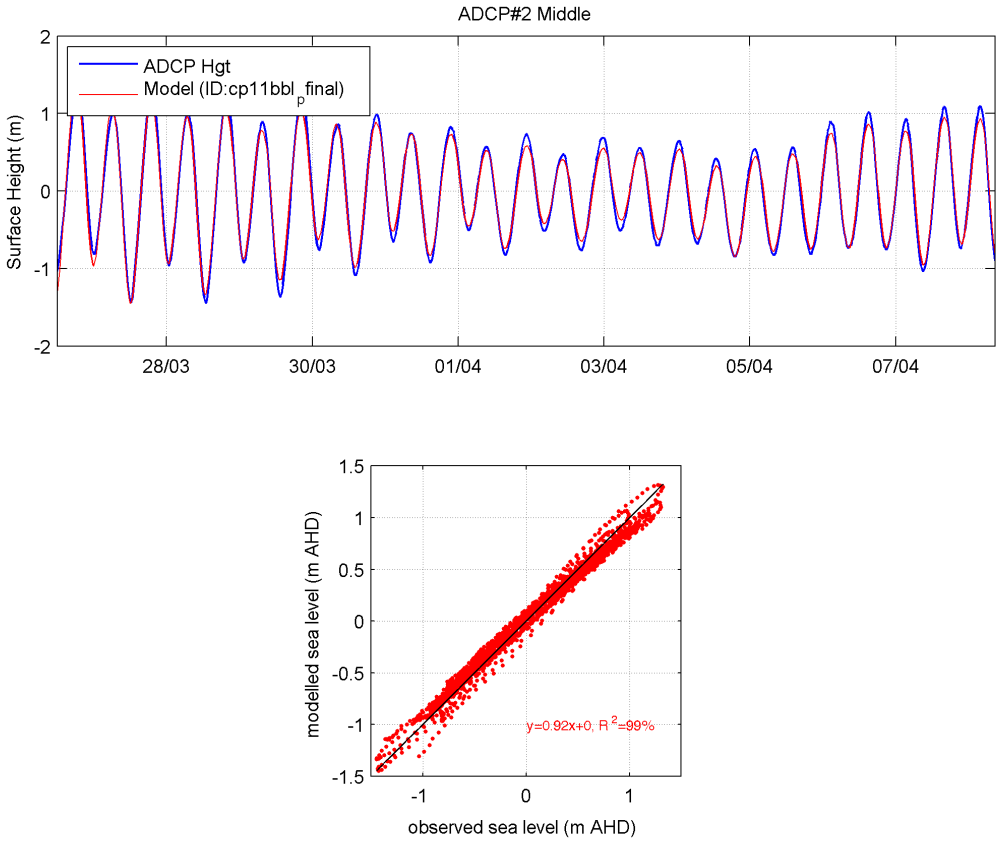

Figure 3.10 Comparison between observed (blue) and modelled (red) surface heights at middle ADCP 2 (Middle).

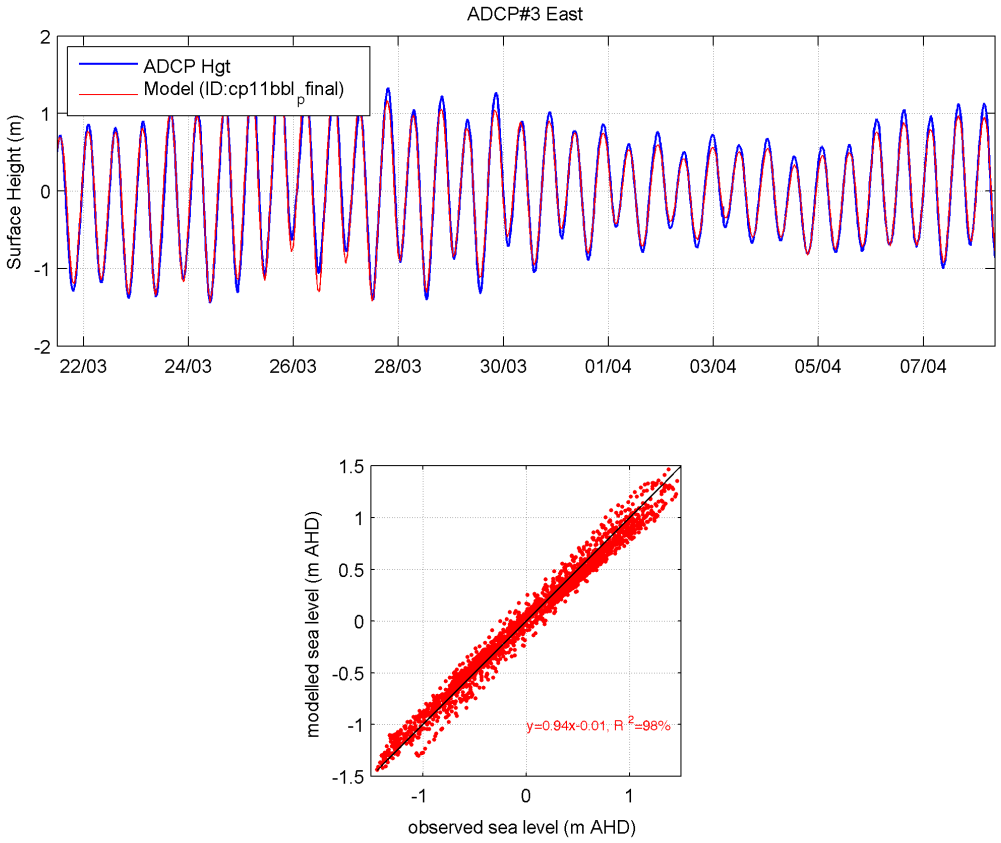

Figure 3.11 Comparison between observed (blue) and modelled (red) surface heights at East ADCP 3 (East).

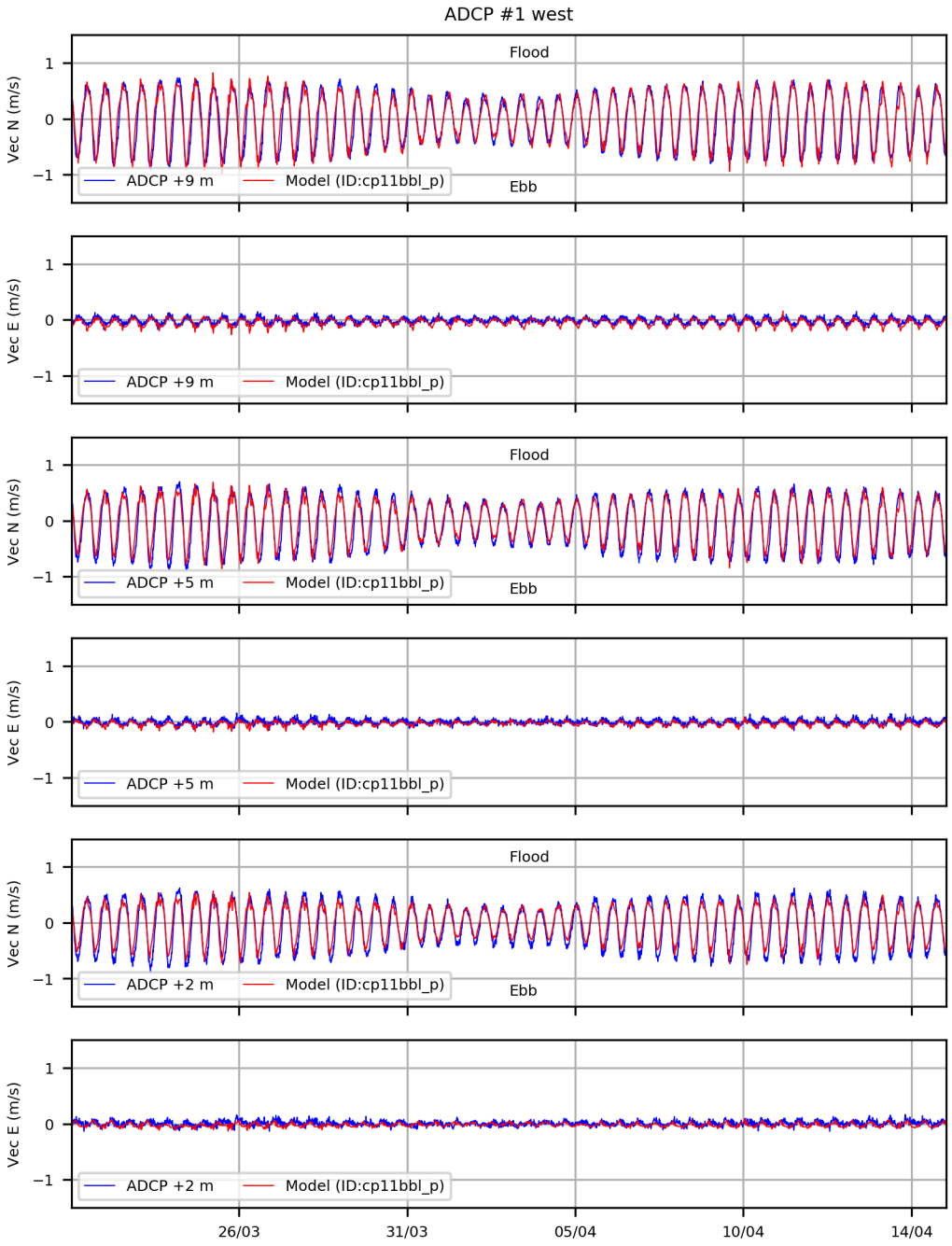

Figure 3.12 Comparison between observed (blue) and modelled (red) north and east current vectors at ADCP 1 (West).

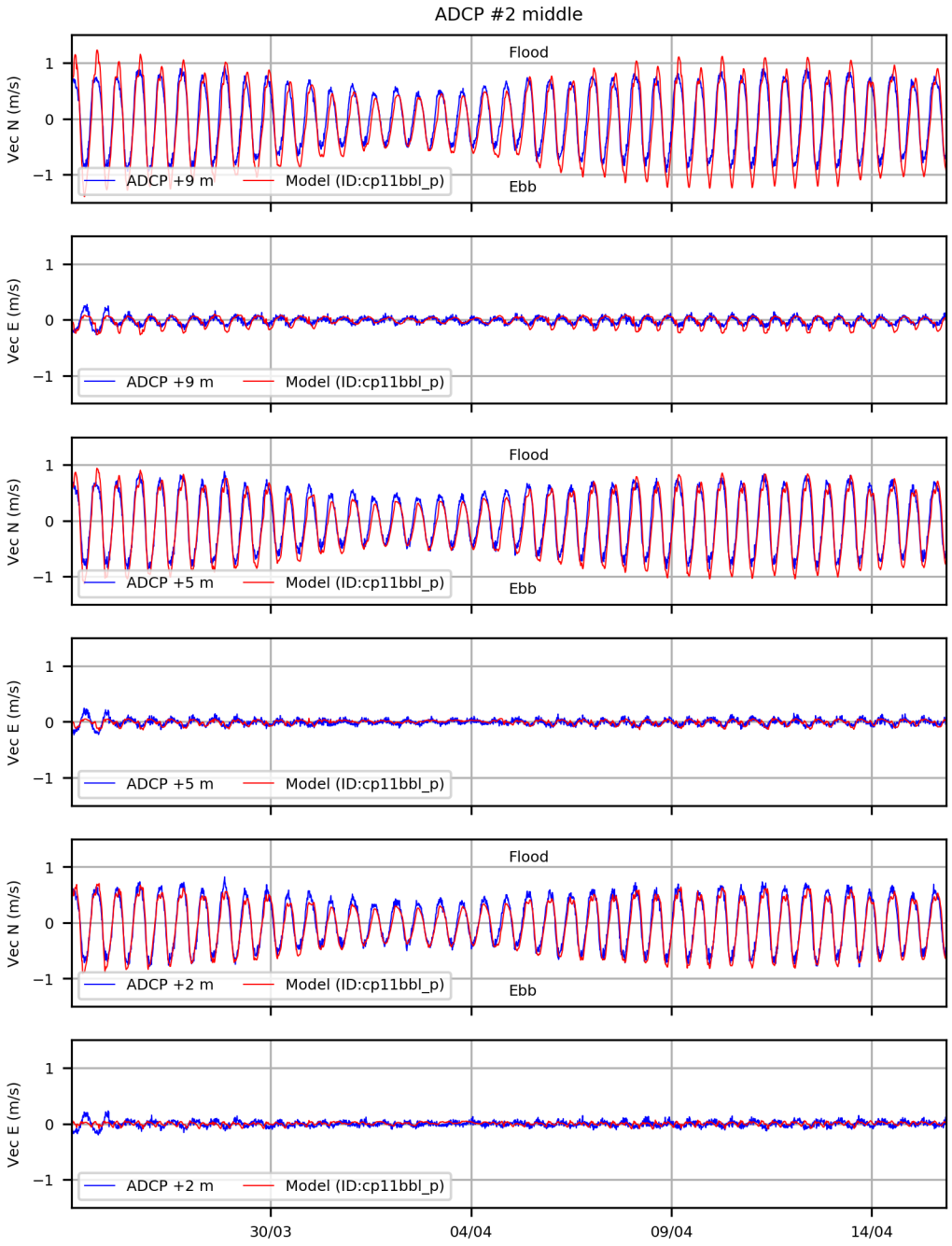

Figure 3.13 Comparison between observed (blue) and modelled (red) north and east current vectors at ADCP 2 (Middle).

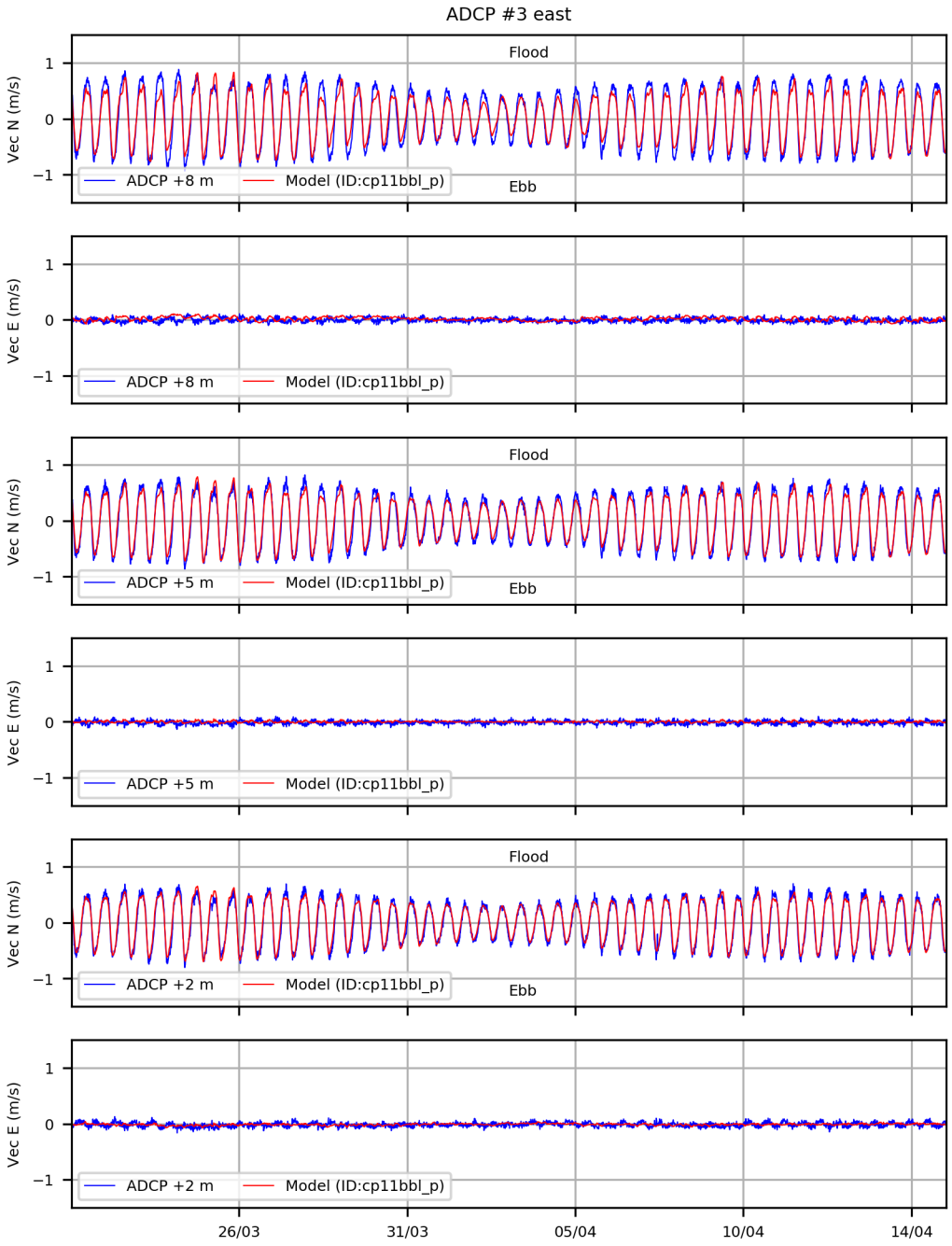

Figure 3.14 Comparison between observed (blue) and modelled (red) north and east current vectors at ADCP 3 (East).

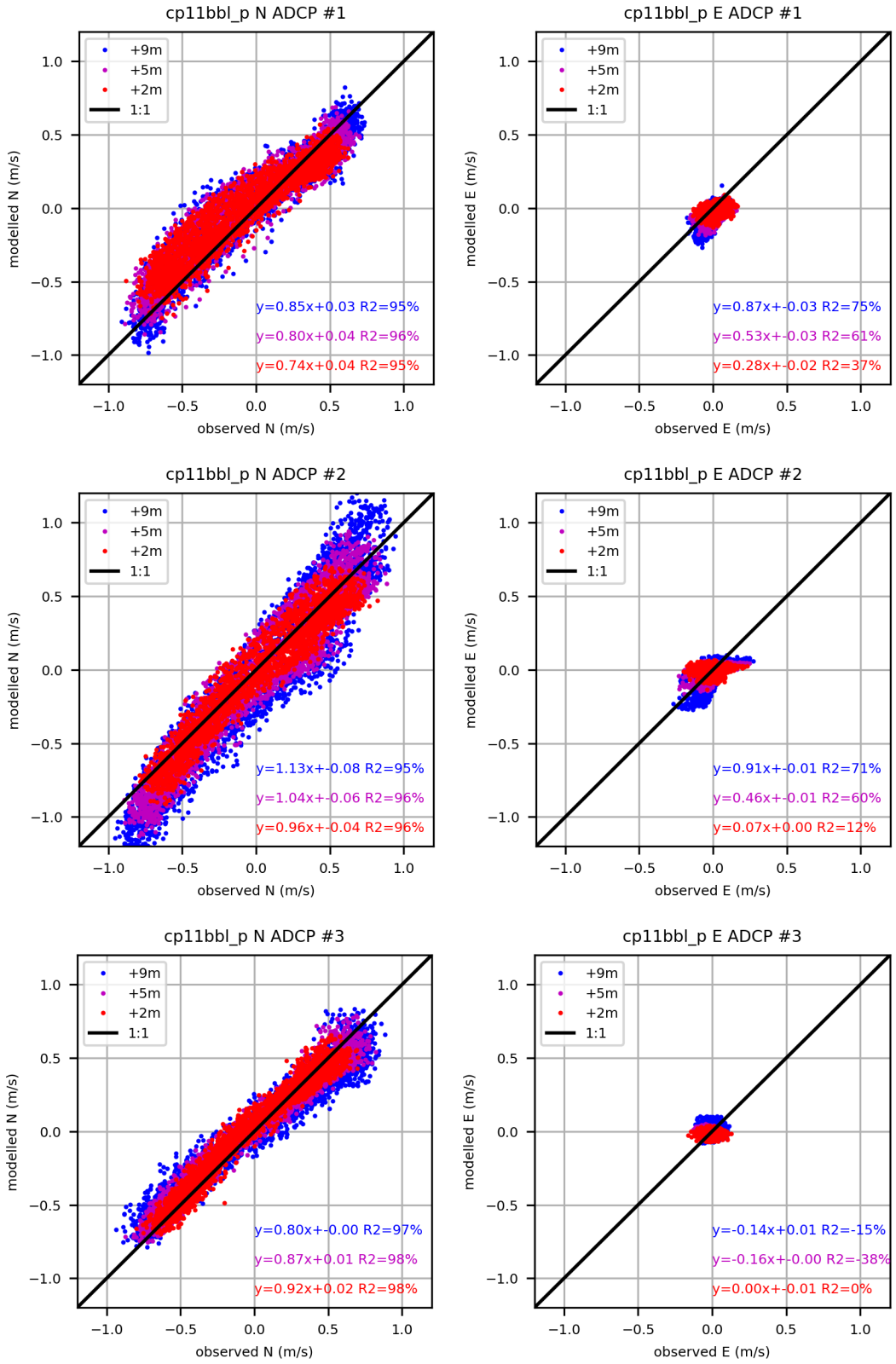

Figure 3.15 Least squares linear fits observed and modelled north and east current vectors at all three ADCP locations.

3.1.4 Simulation X, 50 x 50 m grid

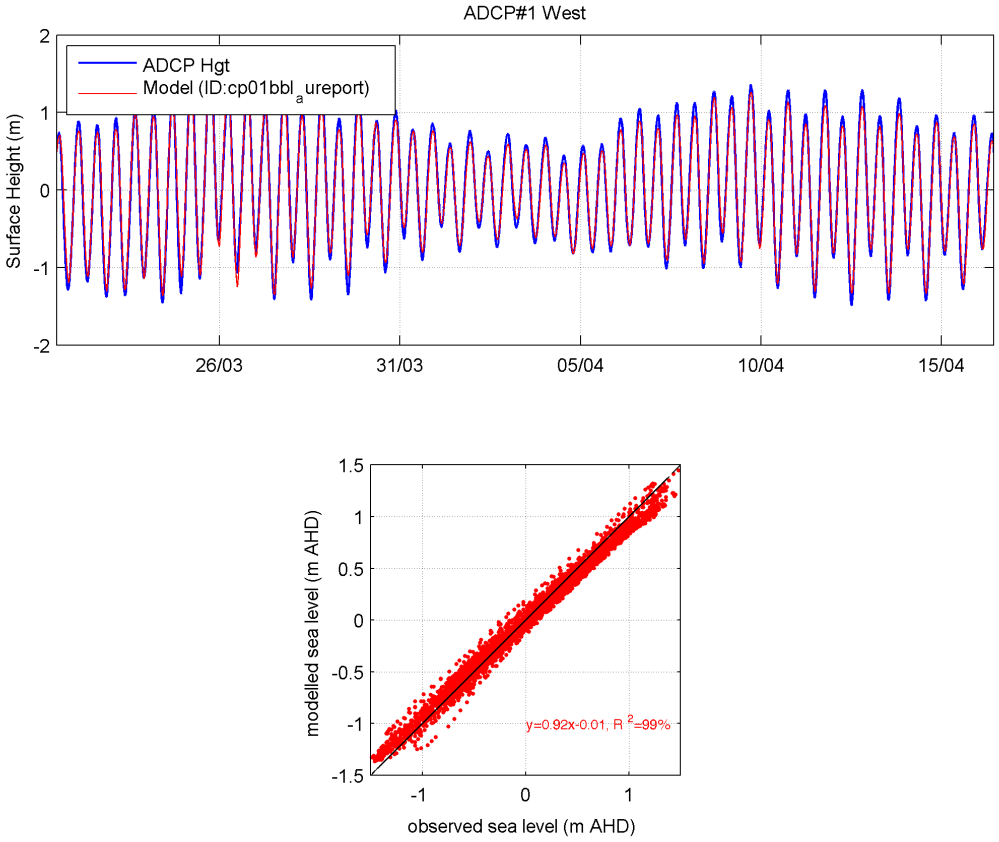

Figure 3.16 Comparison between observed (blue) and modelled (red) surface heights at West ADCP 1 (West).

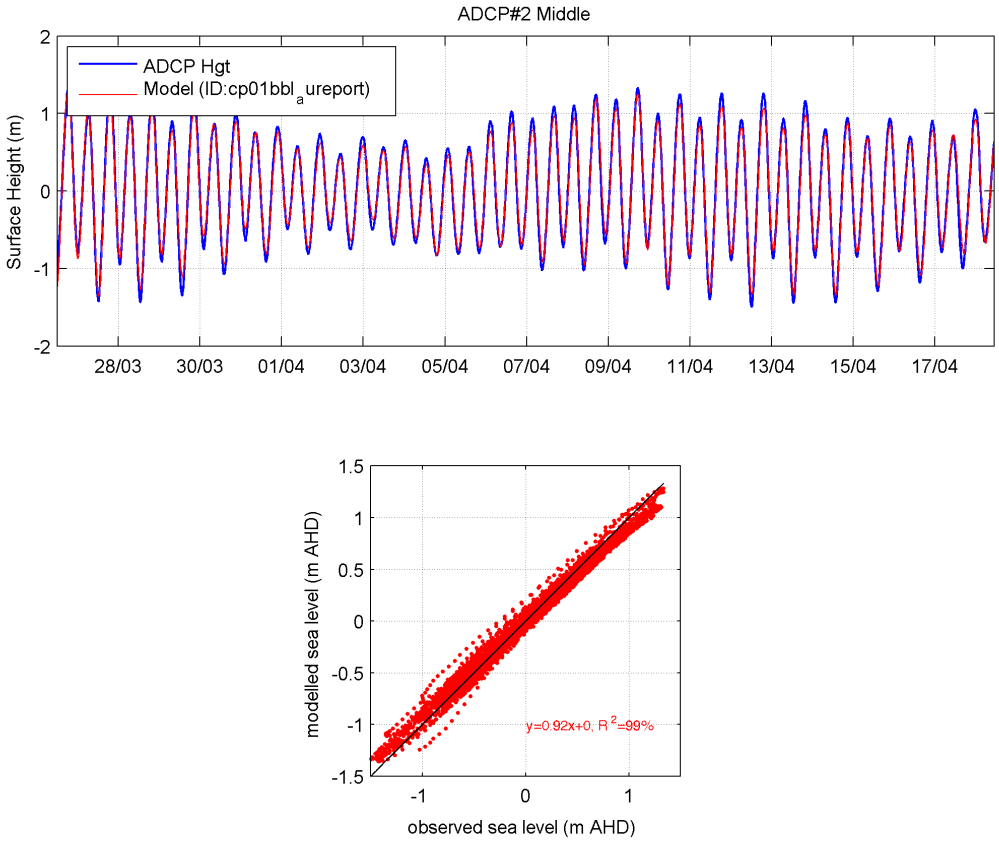

Figure 3.17 Comparison between observed (blue) and modelled (red) surface heights at middle ADCP 2 (Middle).

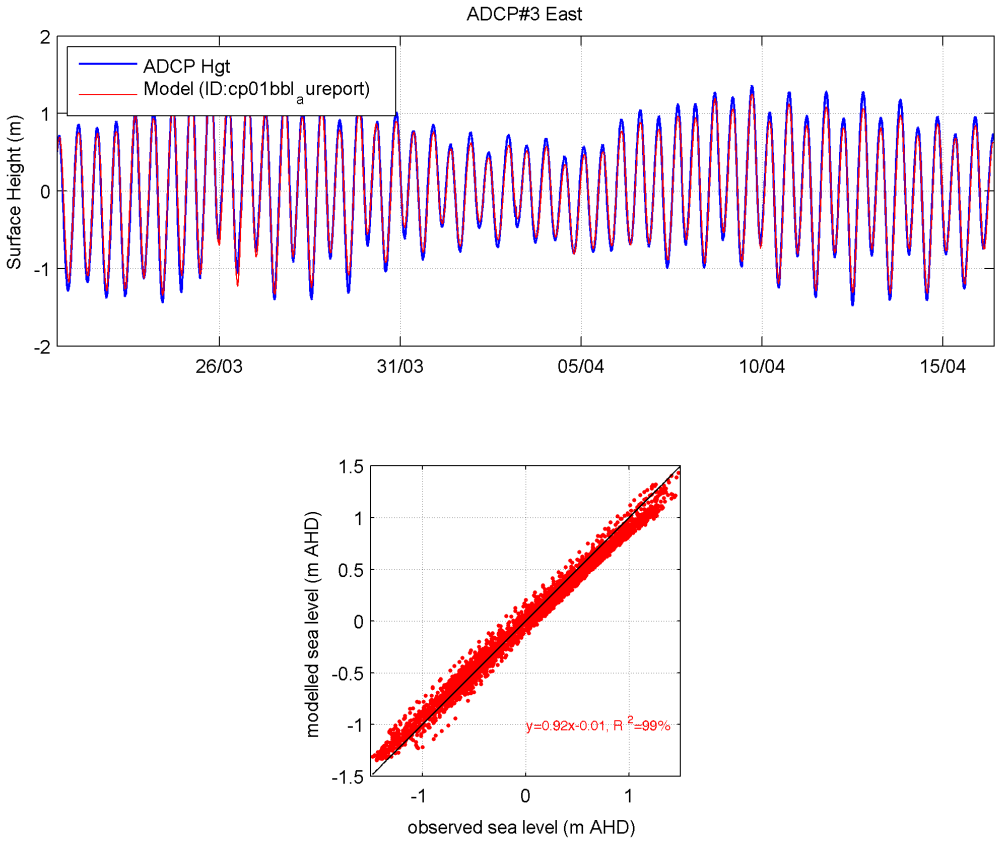

Figure 3.18 Comparison between observed (blue) and modelled (red) surface heights at East ADCP 3 (East).

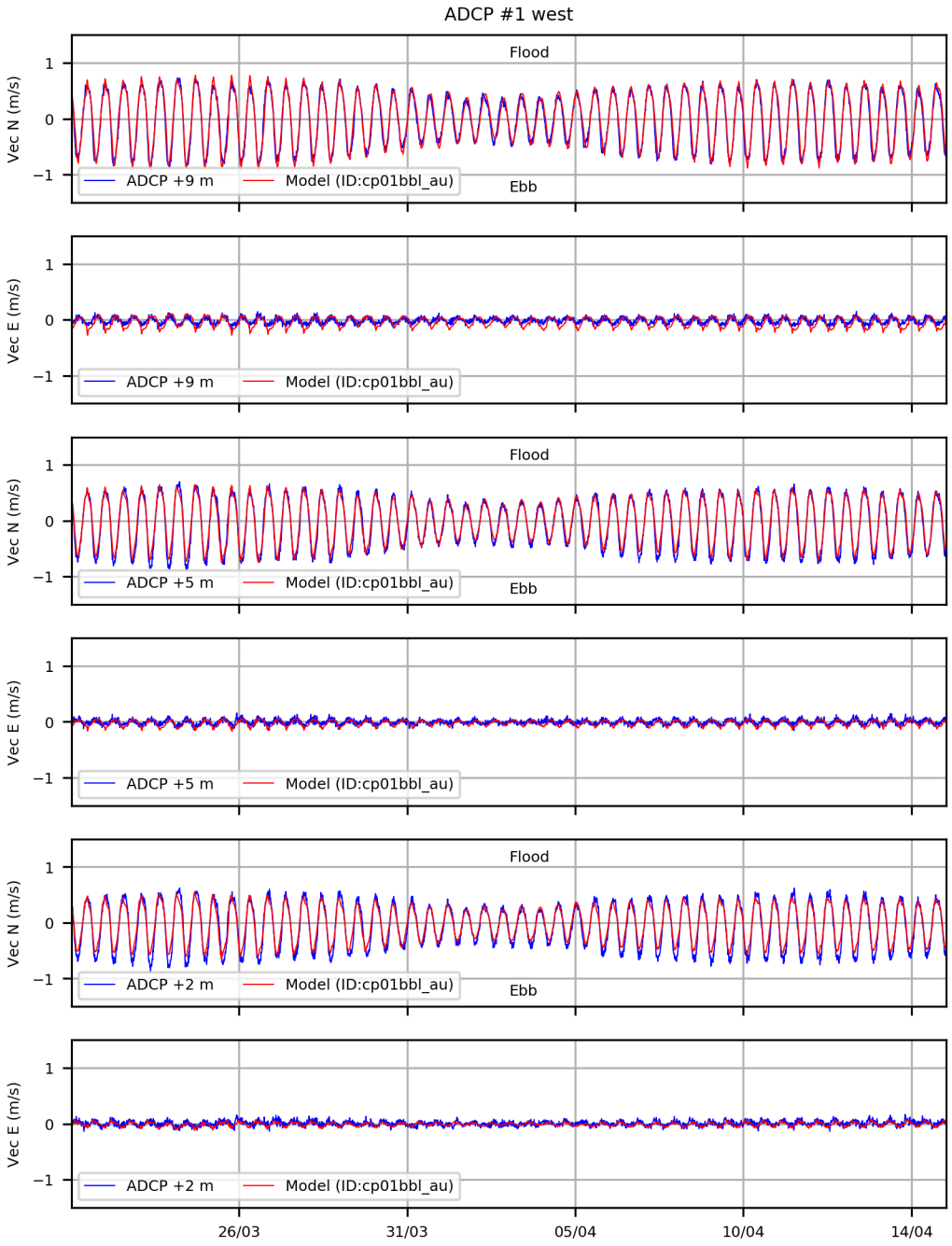

Figure 3.19 Comparison between observed (blue) and modelled (red) north and east current vectors at ADCP 1 (West).

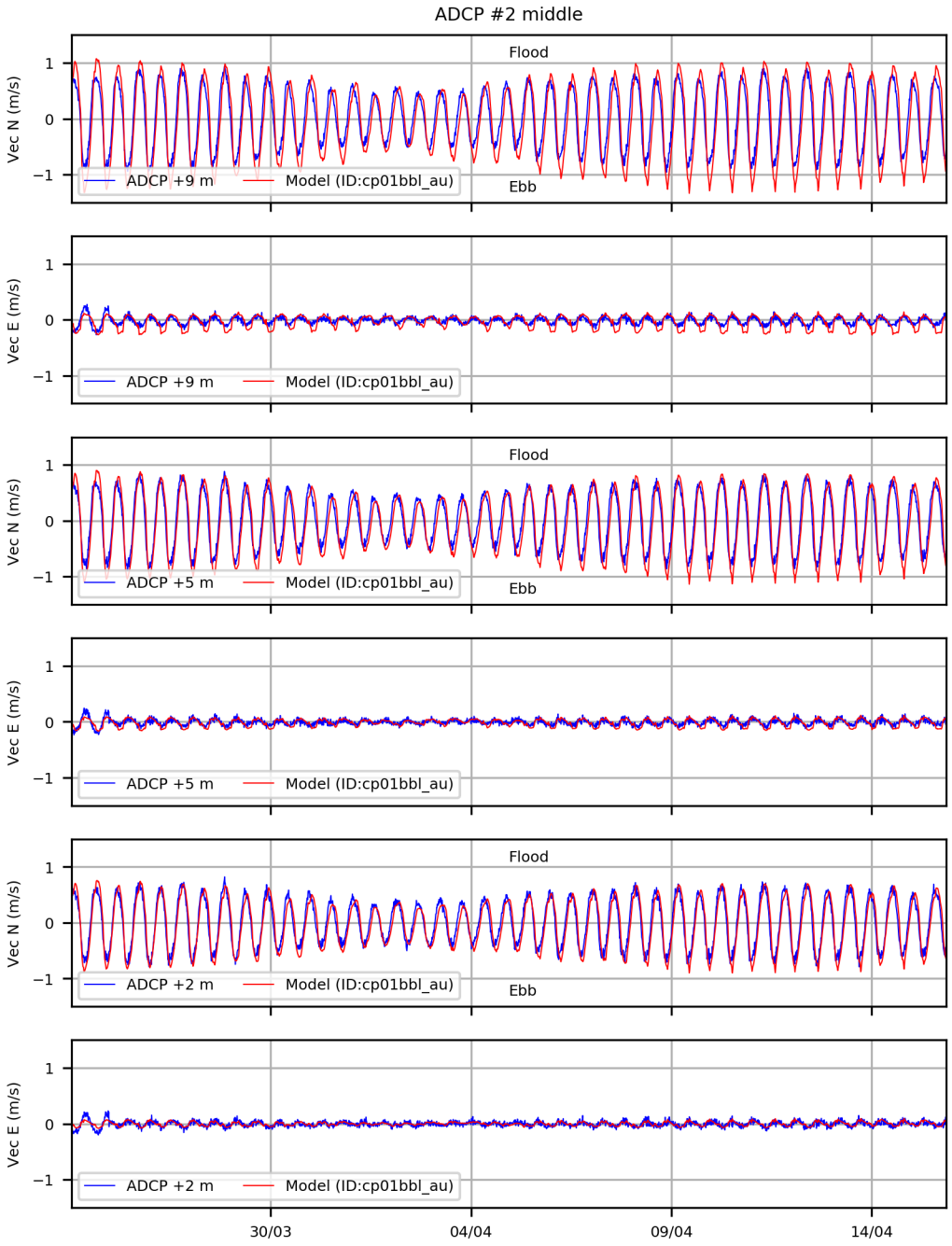

Figure 3.20 Comparison between observed (blue) and modelled (red) north and east current vectors at ADCP 2 (Middle).

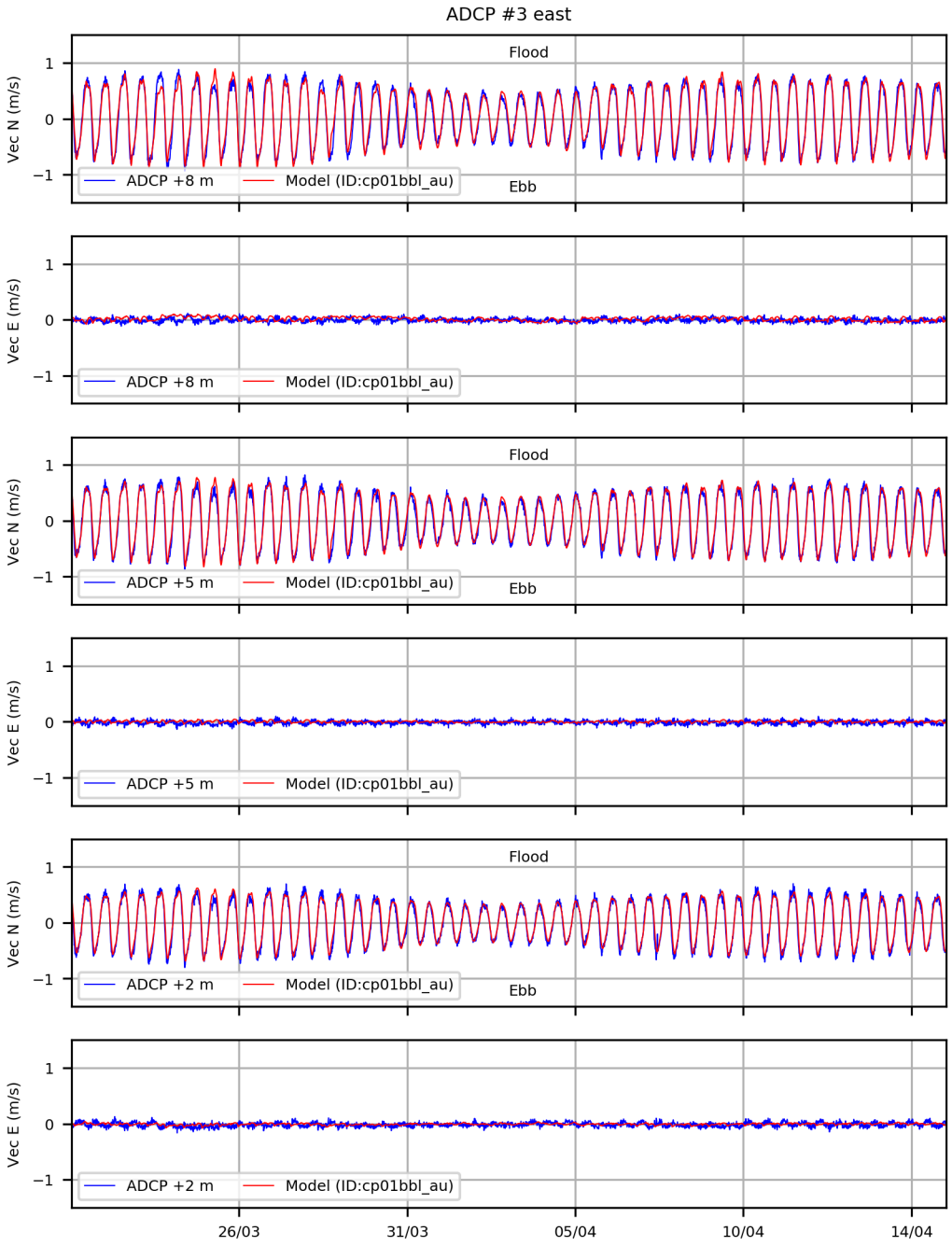

Figure 3.21 Comparison between observed (blue) and modelled (red) north and east current vectors at ADCP 3 (East).

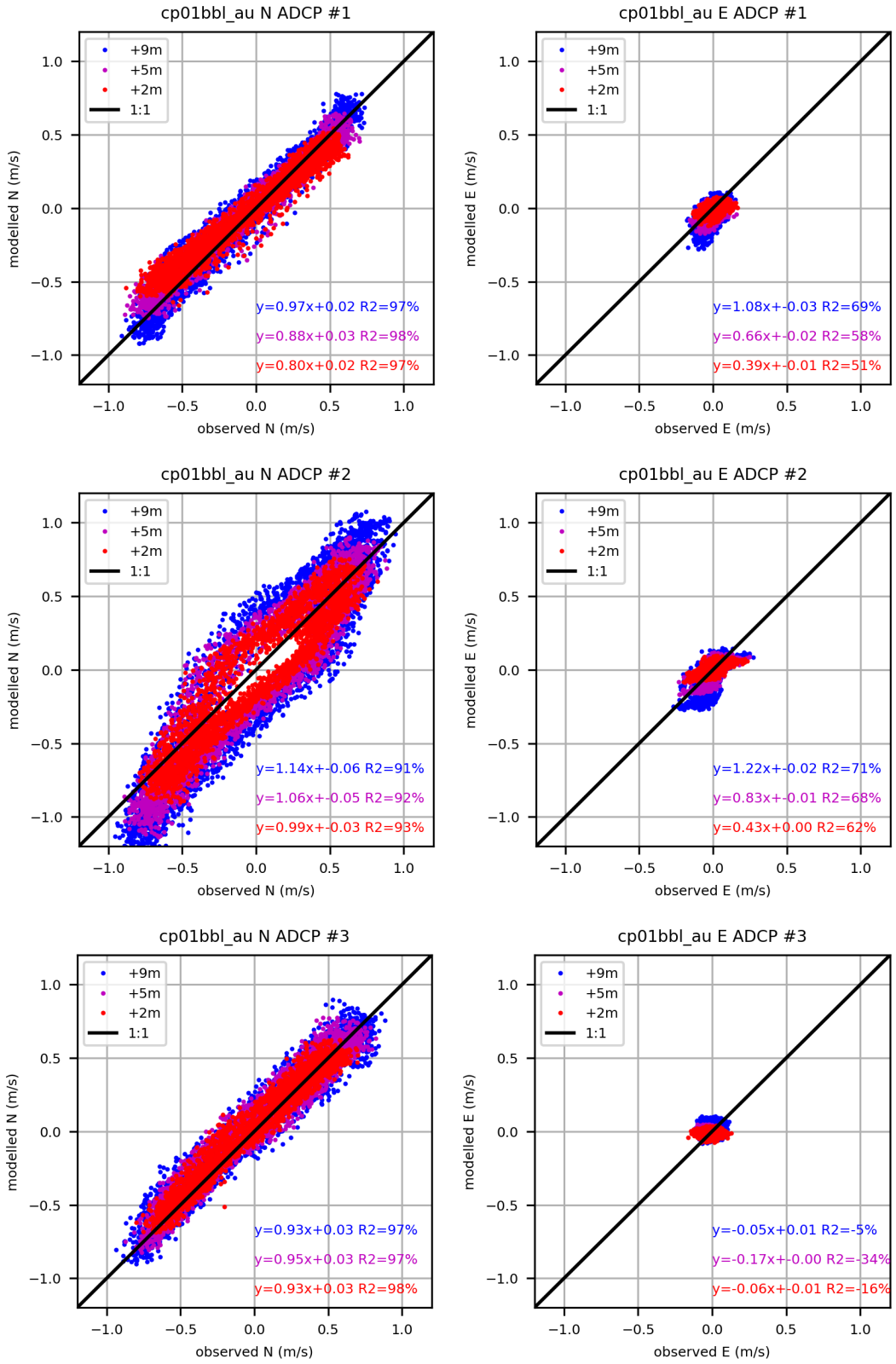

Figure 3.22 Least squares linear fits observed and modelled north and east current vectors at all three ADCP locations.

HydroNumerics

Crib Point LNG Facility

Hydrodynamic Modelling Report

Appendix B
FSRU Discharge Modelling

April 2020

Prepared for CEE Pty Ltd

HydroNumerics Pty Ltd
ABN 87 142 999 246
www.hydronumerics.com.au

NOTICE

DISCLAIMER

The accuracy of information presented in this document is entirely dependent on the accuracy and completeness of supplied information. Hydronumerics Pty Ltd makes no warranty, representation or guarantee with respect to the accuracy and completeness of supplied information, shall have no liability to any person for any errors or omissions in the supplied information, and shall have no liability for loss or damage of any kind suffered or incurred by any person acting in reliance on the information in this document where the loss or damage arises from errors or omissions in the supplied information.

CONTENTS

1 FSRU Vessel 1

1.1 Effect on Local Currents 1

2 FSRU Discharge 7

2.1 Table of Near-field Plume Sensitivity Tests 7
2.2 Results of Near-field Plume Sensitivity Tests 8
2.2.1 Temperature 8
2.2.2 Chlorine 11

1 FSRU Vessel

1.1 Effect on Local Currents

A comparison between simulations with and without the FSRU and LNG tanker were undertaken to assess the potential effects of the moored vessels on the bottom currents near the project site. The simulations were carried out for 24 hours on 2 March 2019 with no discharges using the 20 x 20 m model grid. The FSRU and LNG tanker were approximated to be 40 m wide by 300 m long (i.e. 2 x 15 grid cells) with a draught to 11.5 m moored at Crib Point Jetty Birth 2. When moored together there is no model cell gap between the vessels. The results pf the simulations are illustrated in Figure 1.6 to Figure 1.6.

The results indicate that the presence of the FSRU leads to an increase in bottom currents near and under the vessels. When the FSRU is moored the mean bottom currents on the port side increase to the north and on the starboard side they increase to the south. The increases reach approximately 0.06 m/s in the corners of the vessel. At the bow of the vessel there is a similar magnitude of increase in bottom currents to the west and at the stern there is an increase to the east. The model results with the inclusion of the LNG tanker moored beside the FSRU indicate similar patterns in the changes to the flow around the coupled vessels, with a small amplification of the magnitude of the changes in the mean currents of up to approximately 0.08 to 0.1 m/s.

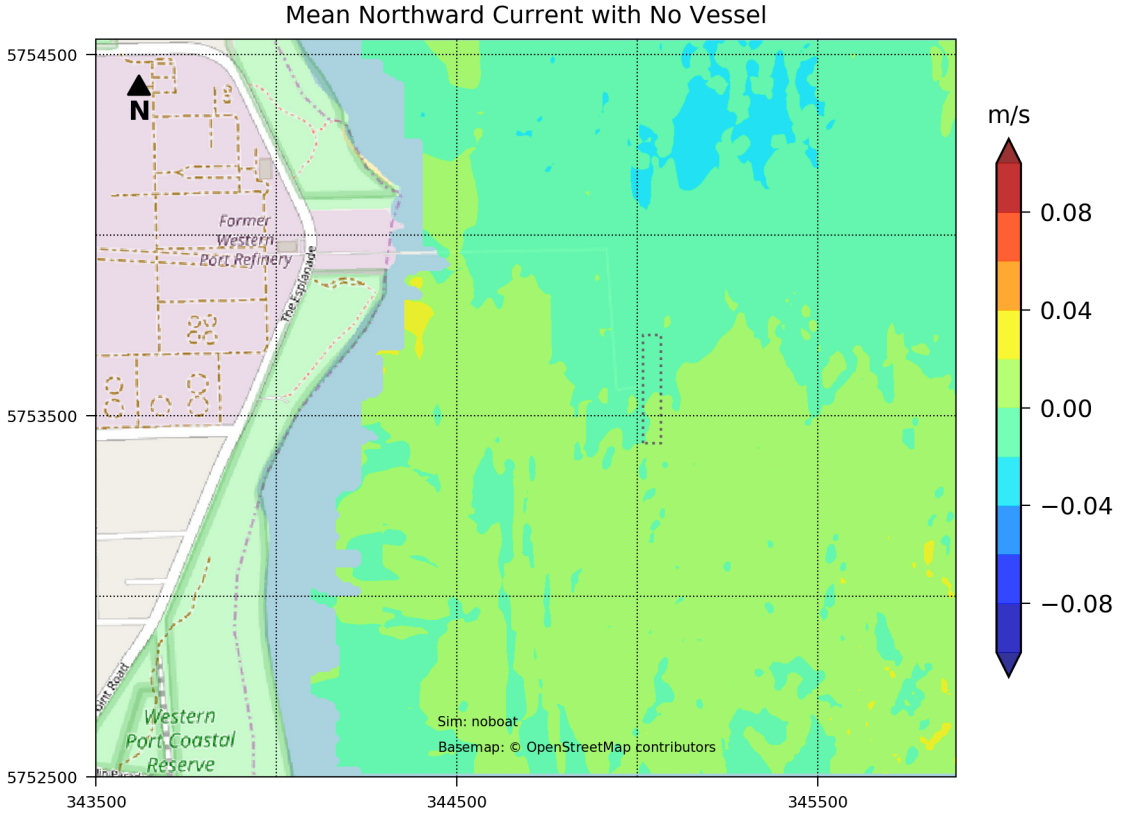

Figure 1.1 Simulated mean northerly currents at the seabed over 24 hours on 2 March 2019 with no vessels moored at Crib Point Jetty.

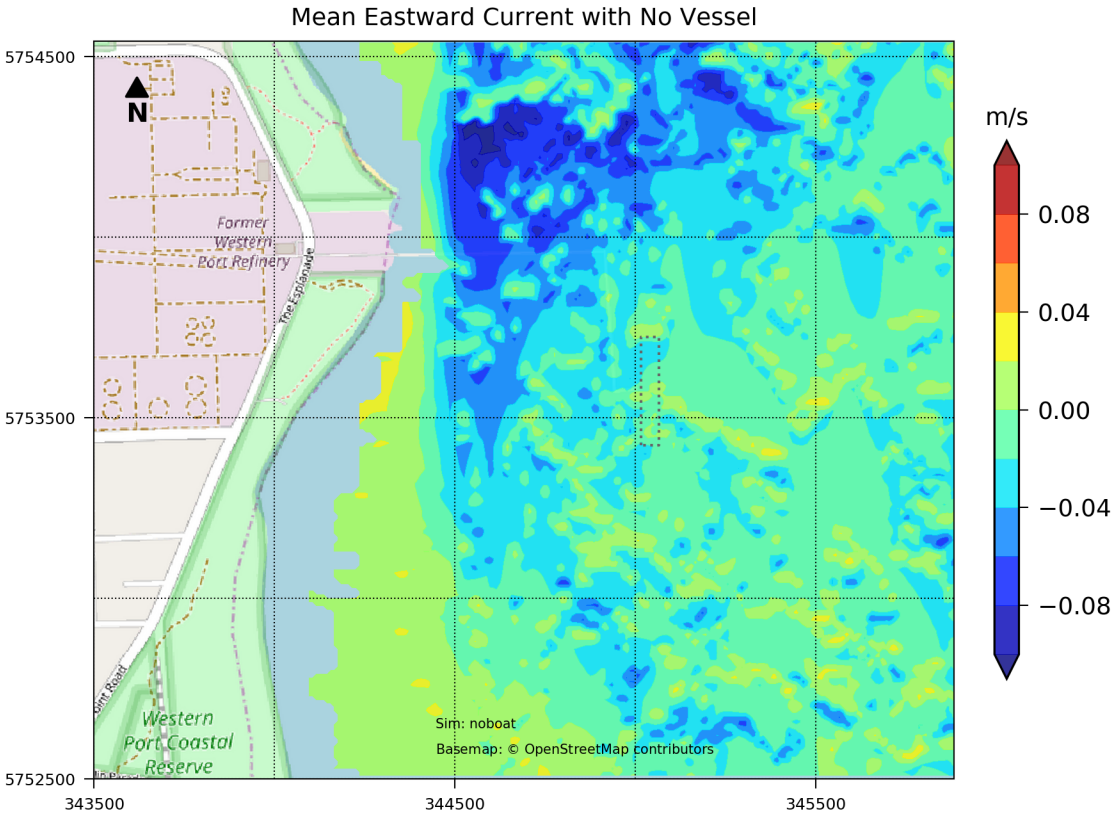

Figure 1.2 Simulated mean easterly currents at the seabed over 24 hours on 2 March 2019 with no vessels moored at Crib Point Jetty.

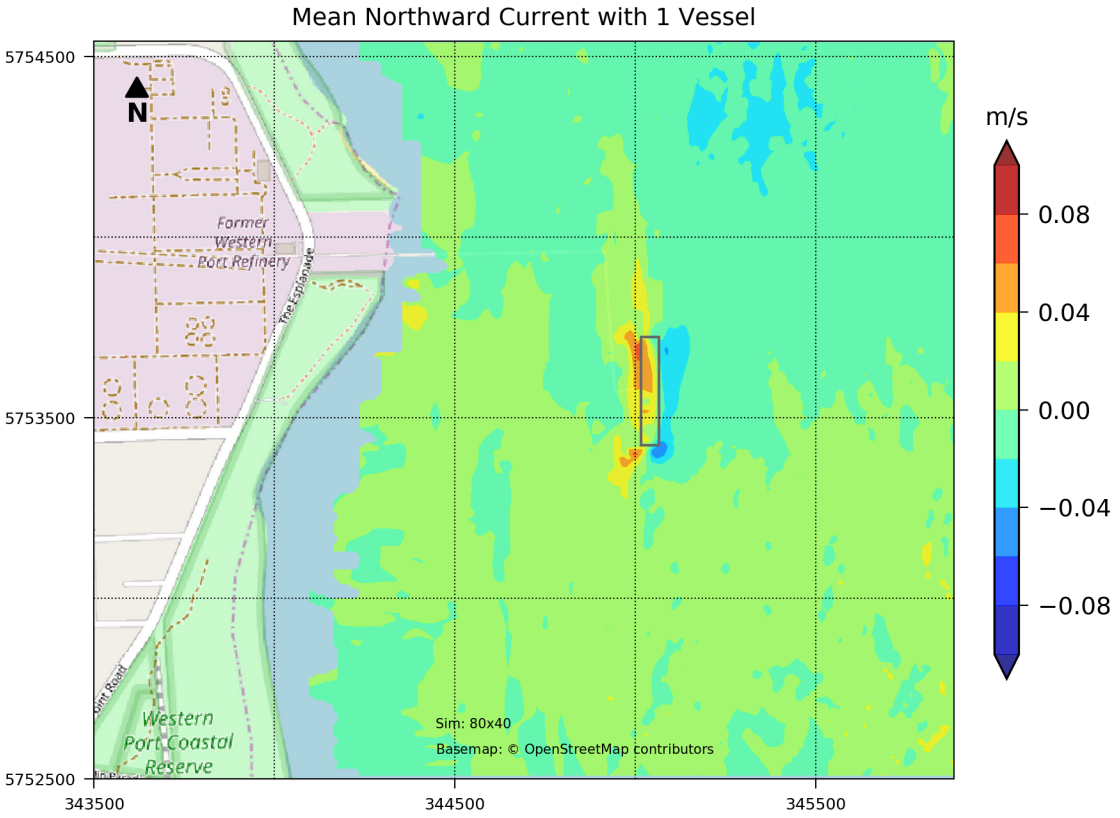

Figure 1.3 Simulated mean northerly currents at the seabed over 24 hours on 2 March 2019 with FSRU moored at Crib Point Jetty.

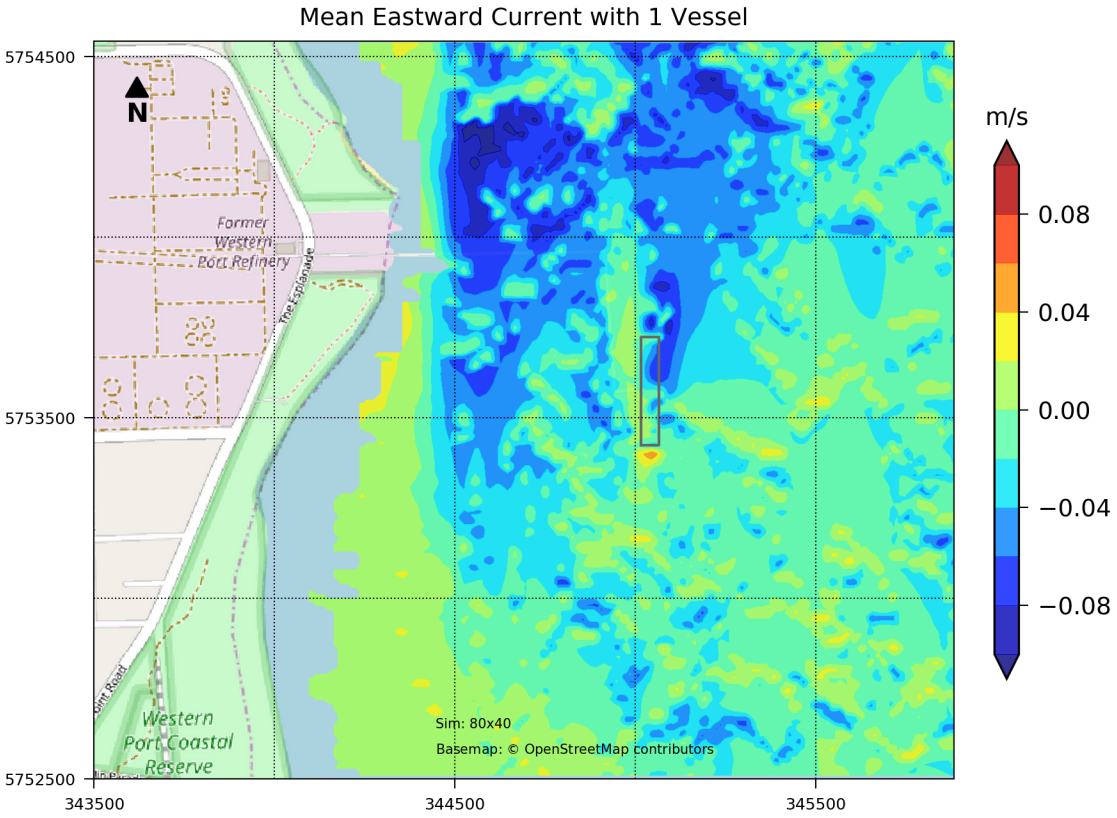

Figure 1.4 Simulated mean easterly currents at the seabed over 24 hours on 2 March 2019 with FSRU moored at Crib Point Jetty.

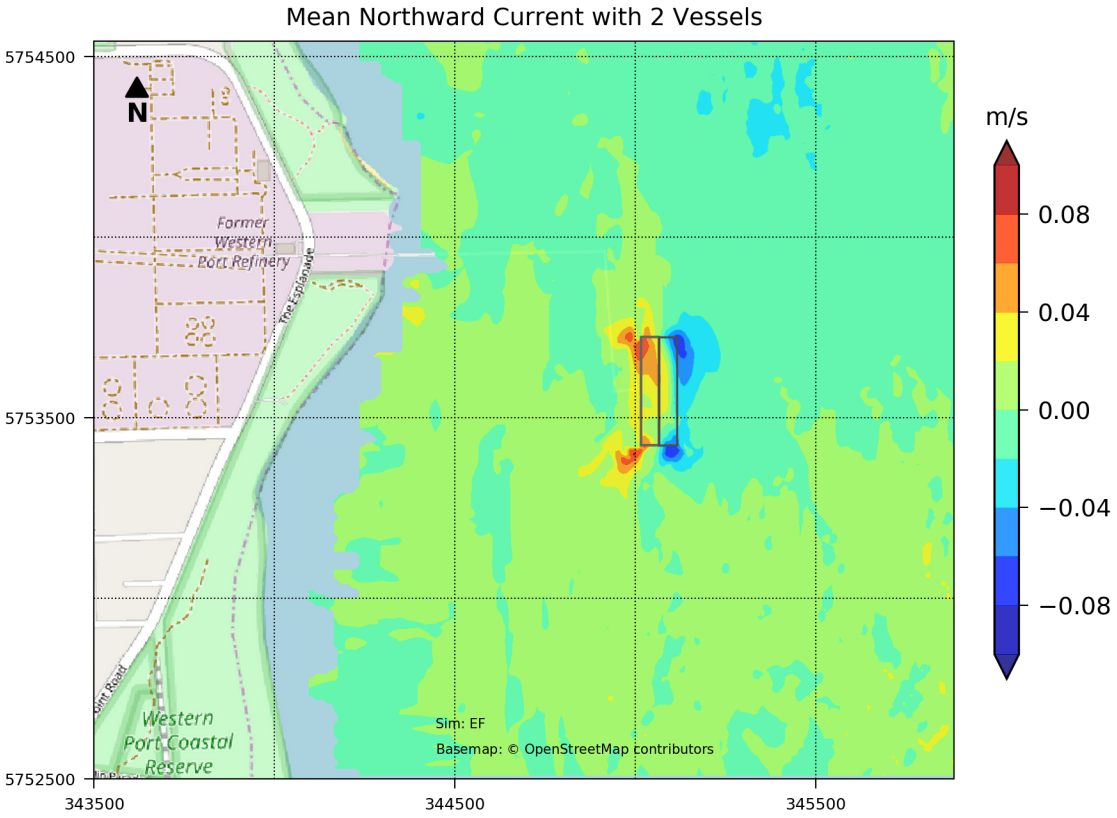

Figure 1.5 Simulated mean northerly currents at the seabed over 24 hours on 2 March 2019 with FSRU and LNG tanker moored at Crib Point Jetty.

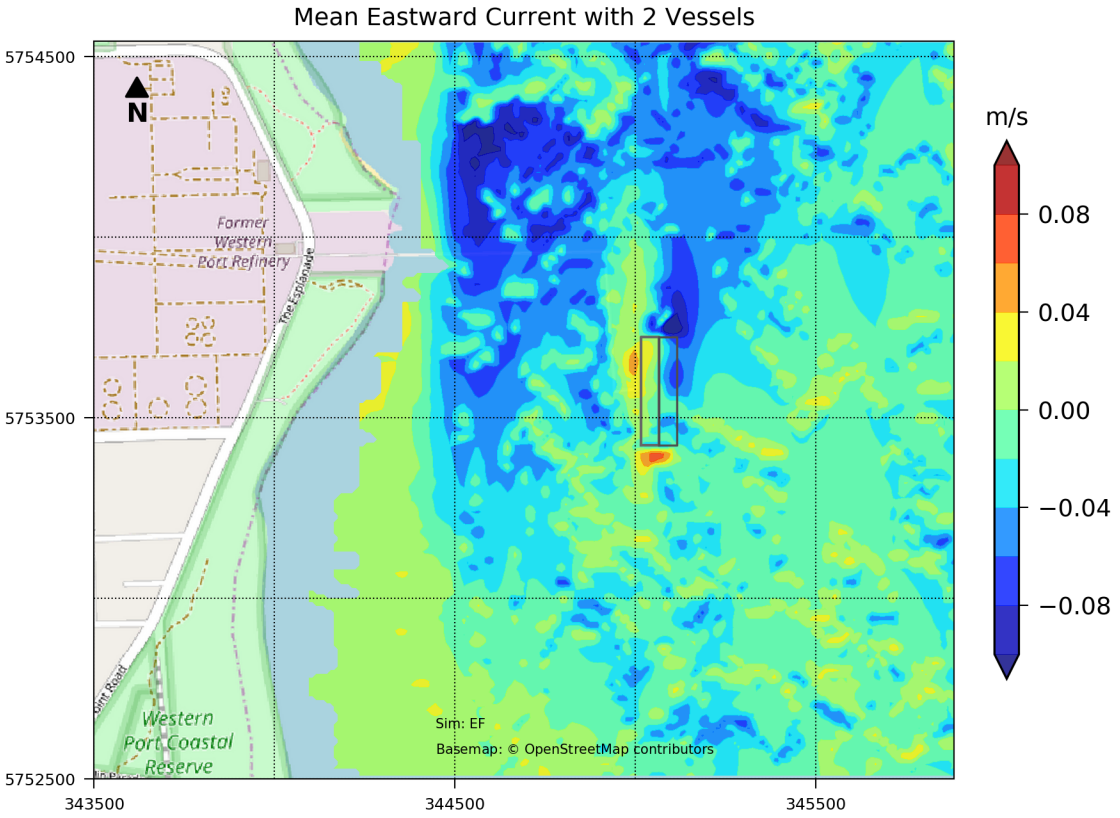

Figure 1.6 Simulated mean easterly currents at the seabed over 24 hours on 2 March 2019 with FSRU and LNG tanker moored at Crib Point Jetty.

2 FSRU Discharge

2.1 Table of Near-field Plume Sensitivity Tests

		Plume location and size						
	Discharge type	**Distance East**	**Lateral** (m)	**Vertical (at slack tide)** (m)	**Slack tide** (m/s)	**Flow** (m^3/s)	**Chlorine** (ug/L)	**Temp.** (^oC)
*I	Open Loop	Function of current	80 x 40	14	< 0.05	5.42	100	-7
V	Open Loop	Function of current	80 x 40	14	< 0.1	5.42	100	-7
VI	Open Loop	Function of current	80 x 40	1	< 0.05	5.42	100	-7
VII	Open Loop	Function of current	80 x 20	14	< 0.05	5.42	100	-7
VIII	Open Loop	Function of current	60 x 40	14	< 0.05	5.42	100	-7
IX	Open Loop	Function of current	60 x 20	14	< 0.05	5.42	100	-7
X	Open Loop	Fixed 10m east	60 x 20 fixed	14	< 0.05	5.42	100	-7

* Base case used for report modelling - March 2019 boundary conditions were used for all simulations.

2.2 Results of Near-field Plume Sensitivity Tests

2.2.1 Temperature

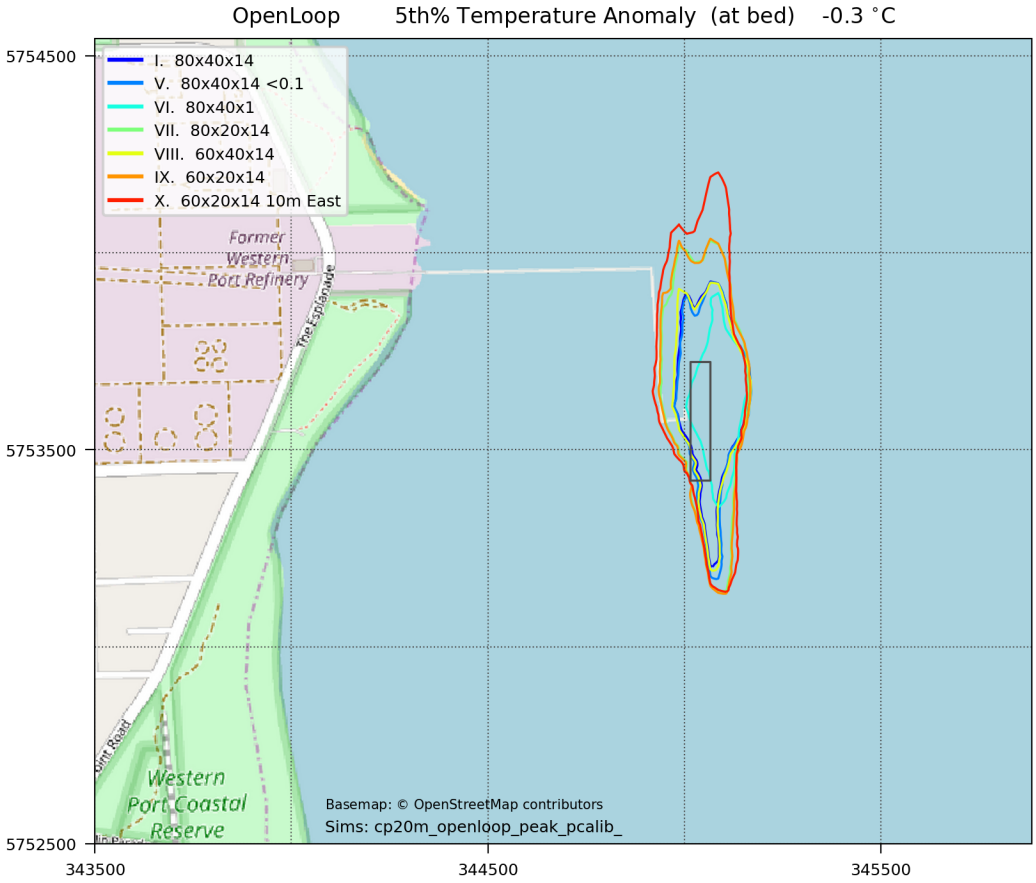

Figure 2.1 -0.3 ºC contour of 5th percentile of temperature decrease at the seabed during over a 28-day simulation at average FSRU discharge.

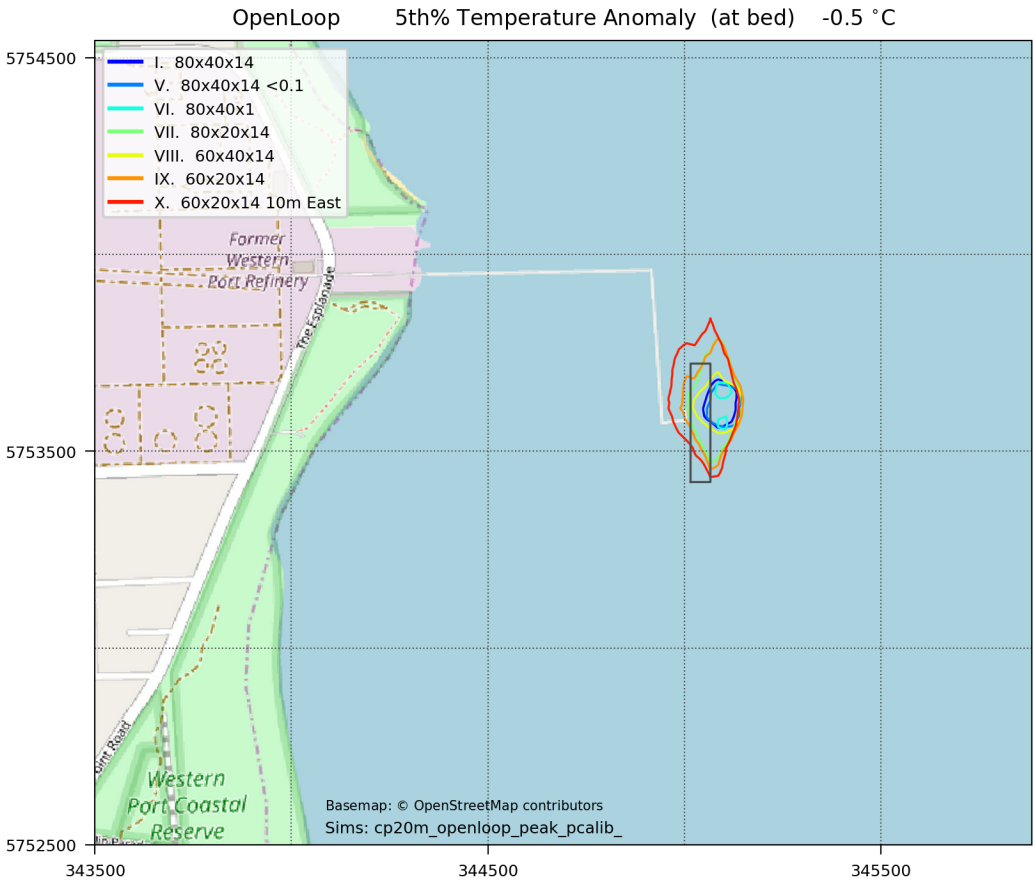

Figure 2.2 -0.5 ºC contour of 5th percentile of temperature decrease at the seabed during over a 28-day simulation at peak FSRU discharge.

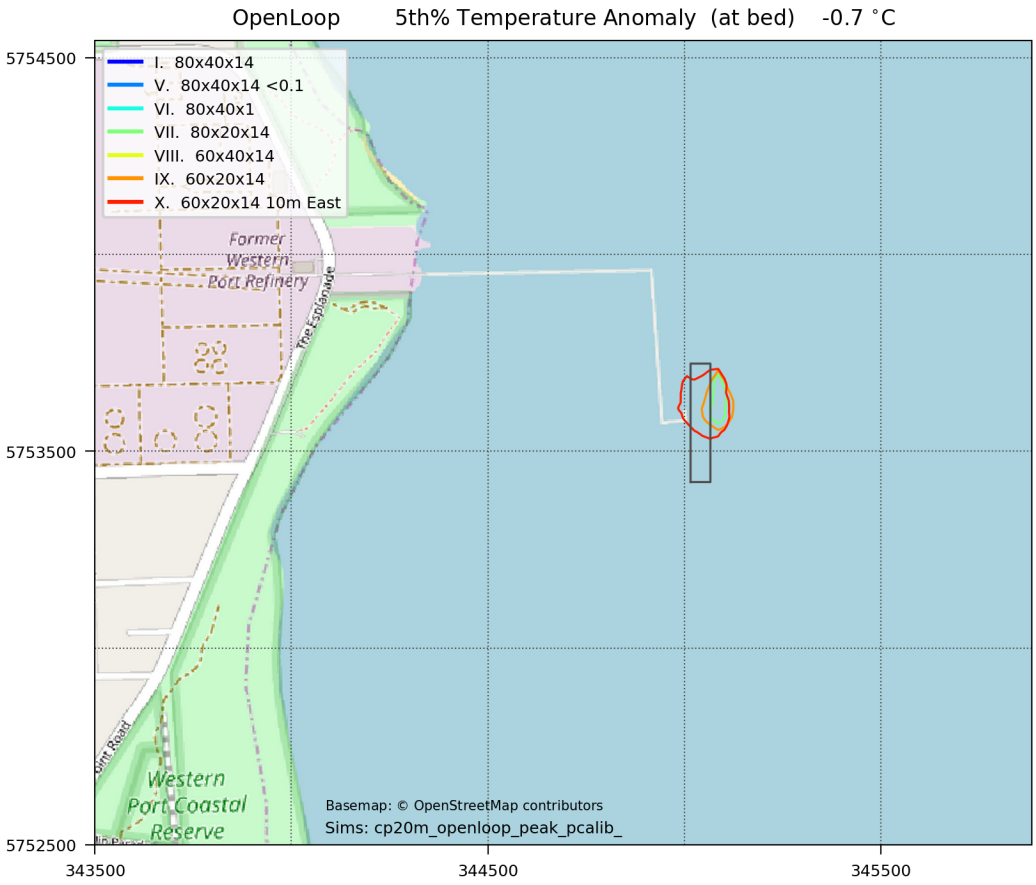

Figure 2.3 -0.7 ºC contour of 5th percentile of temperature decrease at the seabed during over a 28-day simulation at peak FSRU discharge.

2.2.2 Chlorine

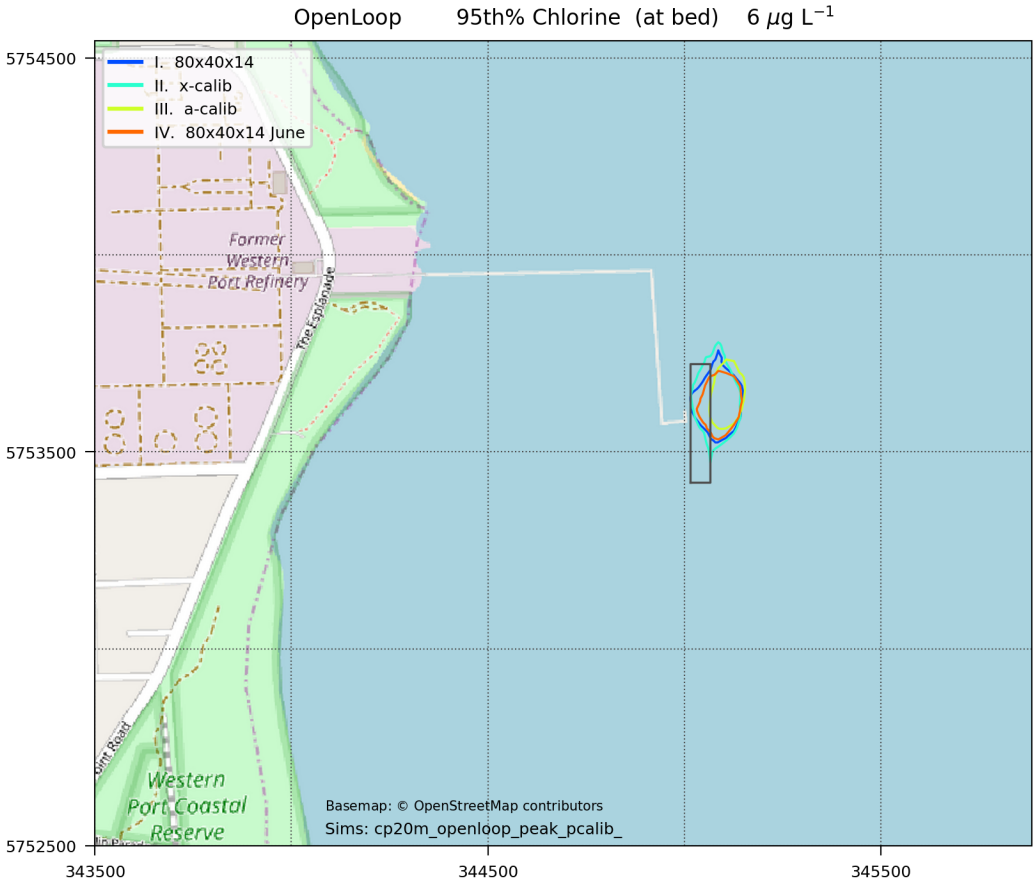

Figure 2.4 95th percentile contour of 6 μg/L chlorine concentration at the seabed over a 28-day simulation at peak FSRU discharge.

HydroNumerics

Crib Point LNG Facility

Hydrodynamic Modelling Report

Appendix C
FSRU Intake Modelling

June 2020

Prepared for CEE Pty Ltd

HydroNumerics Pty Ltd
ABN 87 142 999 246
www.hydronumerics.com.au

NOTICE

DISCLAIMER

The accuracy of information presented in this document is entirely dependent on the accuracy and completeness of supplied information. Hydronumerics Pty Ltd makes no warranty, representation or guarantee with respect to the accuracy and completeness of supplied information, shall have no liability to any person for any errors or omissions in the supplied information, and shall have no liability for loss or damage of any kind suffered or incurred by any person acting in reliance on the information in this document where the loss or damage arises from errors or omissions in the supplied information.

HydroNumerics

CONTENTS

1 Entrainment Sensitivity Simulations 1

1 Entrainment Sensitivity Simulations

Zone	Release Description	Number Released	Percentage Entrainment into FSRU at Peak Production								
			Over 28 Days						Per Day		
			Sea Chest		Total	Max	Ave	North Arm Max	Zone	North Arm	
			West	East							
2	Uniform distribution at the surface during a spring rising tide	5976	0.17	0.59	0.75	0.75	0.66	0.38	0.027	0.014	
	Mixed distribution (lateral and vertical) during spring rising tide	6184	0.15	0.60	0.74						
	Mixed distribution (lateral and vertical) during spring falling tide	4823	0.12	0.52	0.64						
	Uniform distribution at the surface during a neap rising tide	5909	0.05	0.47	0.52						
	Mixed distribution (lateral and vertical) during neap rising tide	7008	0.10	0.59	0.68						
	Mixed distribution (lateral and vertical) during neap falling tide	5609	0.07	0.57	0.64						
3	Uniform distribution at the surface during a spring rising tide	5859	0.05	0.36	0.41	0.41	0.35		0.015		
	Mixed distribution (lateral and vertical) during spring rising tide	4176	0.05	0.31	0.36						
	Mixed distribution (lateral and vertical) during spring falling tide	3657	0.00	0.38	0.38						
	Uniform distribution at the surface during a neap rising tide	5817	0.09	0.26	0.34						
	Mixed distribution (lateral and vertical) during neap rising tide	3776	0.05	0.24	0.29						
	Mixed distribution (lateral and vertical) during neap falling tide	3654	0.08	0.22	0.30						
5	Uniform distribution at the surface during a spring rising tide	4055	0.12	0.12	0.25	0.27	0.26		0.010		
	Mixed distribution (lateral and vertical) during spring rising tide	4036	0.12	0.12	0.25						
	Mixed distribution (lateral and vertical) during spring falling tide	4024	0.15	0.12	0.27						
6	Uniform distribution at the surface during a spring rising tide	9165	0.02	0.08	0.10	0.10	0.09		0.004		
	Mixed distribution (lateral and vertical) during spring rising tide	7881	0.03	0.06	0.09						
	Mixed distribution (lateral and vertical) during spring falling tide	7091	0.01	0.06	0.07						
7	Uniform distribution at the surface during a spring rising tide	5095	0.06	0.18	0.24	0.37	0.17		0.013		
	Mixed distribution (lateral and vertical) during spring rising tide	3137	0.03	0.13	0.16						
	Mixed distribution (lateral and vertical) during spring falling tide	3457	0.00	0.09	0.09						
	Uniform distribution at the surface during a neap rising tide	5189	0.04	0.33	0.37						
	Mixed distribution (lateral and vertical) during neap rising tide	3355	0.00	0.09	0.09						
	Mixed distribution (lateral and vertical) during neap falling tide	3152	0.00	0.06	0.06						
8	Uniform distribution at the surface during a spring rising tide	63921	0.02	0.09	0.11	0.13	0.12		0.005		
	Mixed distribution (lateral and vertical) during spring rising tide	60535	0.02	0.10	0.12						
	Mixed distribution (lateral and vertical) during spring falling tide	62762	0.02	0.11	0.13						
9	Uniform distribution at the surface during a spring rising tide	17527	0.00	0.01	0.01	0.05	0.03		0.002		
	Mixed distribution (lateral and vertical) during spring rising tide	13705	0.00	0.04	0.04						
	Mixed distribution (lateral and vertical) during spring falling tide	14128	0.00	0.05	0.05						
10	Uniform distribution at the surface during a spring rising tide	37445	0.00	0.04	0.05	0.06	0.06		0.002		
	Mixed distribution (lateral and vertical) during spring rising tide	24544	0.01	0.05	0.06						
	Mixed distribution (lateral and vertical) during spring falling tide	17663	0.01	0.05	0.06						